Role of PML-Nuclear Bodies in Human Herpesvirus 6A and 6B Genome Integration.

Vanessa Collin[1], Annie Gravel[1], Benedikt B. Kaufer[2] and Louis Flamand[1,3]

[1]Division of Infectious Disease and Immunity, CHU de Québec Research Center, Quebec City, Quebec Canada, G1V 4G2; [2]Institut für Virologie, Freie Universität Berlin, Berlin, Germany; [3]Department of microbiology, infectious disease and immunology, Faculty of Medicine, Université Laval, Quebec City, Québec, Canada, G1V 0A6

*Corresponding author:

E-mail: Louis.Flamand@crchudequebec.ulaval.ca

Abstract

Human herpesviruses 6A and 6B (HHV-6A/B) are two betaherpesviruses that readily integrate their genomes into the telomeres of human chromosomes. To date, the cellular or viral proteins that facilitate HHV-6A/B integration remain elusive. In the present study, we demonstrate that the immediate early protein 1 (IE1) of HHV-6A/B colocalizes with telomeres during infection. Moreover, IE1 associates with PML-NBs, a nuclear complex that regulates multiples cellular mechanism including DNA repair and antiviral responses. Furthermore, we could demonstrate that IE1 targets all PML isoforms and that both proteins colocalize at telomeres. To determine the role of PML in HHV-6A/B integration, we generated PML knockout cell lines using CRISPR/Cas9. Intriguingly, in the absence of PML, the IE1 protein could still localize to telomeres albeit less frequently. More importantly, HHV-6A/B integration was impaired in the absence of PML, indicating that it plays a role in the integration process. Taken together, we identified the first cellular protein that aids in the integration of HHV-6A/B and shed light on this targeted integration mechanism.

Author summary

Human herpesviruses type 6A and 6B are relatively common viruses whose infections can be life threatening in patients with a compromised immune system. A rather unique feature of these viruses is their ability to integrate their genome in human chromosomes. Integration takes place is a specialized region of the chromosomes known as telomeres, a region that controls cellular lifespan. To date, the mechanisms leading to HHV-6A and HHV-6B integration remain elusive. Our laboratory has identified that the IE1 protein of

40 HHV-6A and HHV-6B target the telomeres. Moreover, we have shown that IE1 associates
41 with a cellular protein, PML, that is responsible for the regulation of important cellular
42 mechanisms such as the life span of cells and DNA repair. Hence, we studied the role of
43 PML in HHV-6 integration. Our study demonstrates that in absence of PML, the HHV-6A
44 and HHV-6B integrate 50-70% less frequently. Thus, our study unveils the first cellular
45 protein involved in HHV-6A and HHV-6 chromosomal integration.
46
47

Introduction

Human herpesviruses type 6A and 6B (HHV-6A/B) are members of the *betaherpesvirinae* that were isolated in the 1980's. In 2013, the International Committee on Taxonomy of Viruses recognized HHV-6A and HHV-6B as distinct viral species (1). HHV-6B is known as the etiologic agent of *exanthem subitum,* a childhood disease whose symptoms include, fever, occasional skin rash and respiratory distress (2). HHV-6A is much less characterized than HHV-6B. Considering that many HHV-6A/B proteins share 90-95% homology, the symptoms of primary HHV-6A infections are likely lessened in part due to cross-protective immunity developed against HHV-6B. Upon primary infection, HHV-6A/B establish latency like all herpesviruses. During latency, most herpesviruses maintain their genome in a circularized form (episome). The viral episomes are generally tethered to the human chromosomes, ensuring transmission to daughter cells following cell division (3), (4). However, to date, the presence of HHV-6A/B episomes during latency have yet to been demonstrated.

Despite the fact that no episomes of HHV-6A/B have been reported, both viruses can reactivate and cause secondary infections. In healthy subjects, HHV-6B reactivation is mostly subclinical and controlled by the immune system. However, in immunocompromised individuals, HHV-6B reactivation can be problematic and occasionally life-threatening (5),(6),(7). In case of HHV-6A, several reports have associated the virus with neurodegenerative diseases such as multiple sclerosis and more recently with Alzheimer's disease (8), (9), (10), (11). In spite of their pathological differences, both HHV-6A and HHV6B can readily integrate their genomes into host

chromosomes (12), (13), (14). HHV-6A/B integration can take place in various chromosomes but invariably occurs within the telomeric region (12), (13), (14). In 1993, Luppi et *al* reported three cases of individuals with telomeric integration of HHV-6A/B (13). In 1999, Daibata et *al* subsequently demonstrated that chromosomally-integrated HHV-6 can be inherited (12). Subjects with inherited chromosomally-integrated HHV-6A/B (iciHHV-6A/B) have at least one (occasionally 2 or 3) copy of the viral genome present in every somatic cells, with the viral genome transmitted to 50% to their children (15), (16). Viral integration into telomeres could be an alternative latency mechanism for HHV-6A/B. In support, the integrated HHV-6A/B genomes are generally intact and conserved without any gross rearrangements or mutations (17). Furthermore, integrated HHV-6A/B genomes can express genes and lead to complete viral reactivation (18)(19),(20),(7). Reactivation of HHV-6A/B can be life threatening for immunocompromised hosts.

Telomeres are non-coding $(TTAGGG)_n$ hexanucleotides present at the chromosome termini and contain a single-stranded 3' extension of 30-500 G rich nucleotides. They protect chromosomes against the loss of genetic information, which would result in premature cell senescence and prevent the recognition of chromosome ends by the DNA damage response (DDR) machinery. The telomere end forms a t-loop (22),(23) that is maintained by a complex of 6 proteins, the shelterin proteins (24), (25) that protect the chromosomes against DNA damage response. The HHV-6A/B genome is about 160 kilobase pairs (kbp) in length and contains a unique region (U) with close to 100 open reading frames (26), (27), (28). This U region is flanked by identical direct repeat regions

94 (DR_L and DR_R) of 8-9 kbp that contain telomere sequences identical to human telomeres
95 at both ends (27), (29). Wallaschek and al. recently demonstrated that these telomeric
96 sequences facilitate integration of HHV-6A into host telomeres (30). This indicated that
97 integration is likely mediated by homologous DNA recombination events. To date, no viral
98 or cellular proteins have been identified that are involved in HHV-6A/B integration.
99
100 An interesting candidate involved in viral integration is the immediate-early protein 1 (IE1)
101 of HHV-6A/B, which can be transcribed without *de novo* protein synthesis (31). The IE
102 proteins of herpesviruses regulate early genes and plays an important role in the initiation
103 of lytic virus replication. Moreover, they establish a favorable environment by
104 manipulating PML-Nuclear bodies (PML-NBs), which are part of the cellular antiviral
105 defense (32), (33), (34). In the context of an infection, PML-NBs have been shown to
106 repress replication of various viruses with its components SP-100 and DAXX. PML-NBs
107 are found mostly in the nucleus and contain large quantities of the PML protein (35), (36).
108 Some viruses have developed ways to overcome this antiviral mechanism by degrading or
109 manipulating PML-NBs. For example, herpes simplex virus 1 (HSV-1) encodes the E3
110 ligase ICP0 that conjugates ubiquitin to PML and induces its degradation (37), (38). Human
111 cytomegalovirus (hCMV) IE1 de-SUMOylates PML-NBs resulting in PML redistribution
112 (39). In contrast, HHV-6A/B infection does induce dispersal of PML-NBs but reduces and
113 increases their size (32), (33), (40). Intriguingly, HHV-6B IE1 has been shown to
114 colocalize with PML during infection (32), (33) however, the role of this PML-IE1
115 interaction remains unknown.
116

Considering that 1) PML is located at telomeres, 2) PML-NBs associate with proteins involved in homologous recombination and 3) viral integration occurs at telomeres, we hypothesize that PML likely plays a role in HHV-6A/B chromosomal integration. We addressed this hypothesis and could demonstrate that HHV-6A/B IE1 not only localizes with PML, but also the host telomeres. In addition, we could demonstrate that PML indeed plays a role in HHV-6A/B integration.

Materials and methods

Cell lines and viruses

HeLa cells with long telomeres (Hela LT) (41) and HEK293T (ATCC, Manassas, VA, USA) were cultured in Dulbecco's modified Eagle's medium (DMEM; Corning Cellgro, Manassas, VA, USA) supplemented with 10% fetal bovine serum (FBS) (Thermo Fisher Scientific, Waltham, MA, USA), nonessential amino acids (Corning Cellgro), HEPES, sodium pyruvate (Wisent Inc., St-Bruno, Québec, Canada), and 5 µg/ml plasmocin (Invitrogen, San Diego, CA, USA). U2OS (osteosarcoma) cells (ATCC) were cultured in the same medium but supplement with 10% of Nu serum (Corning Cellgro) instead of FBS.

Plasmids

Expression vectors for HHV-6A IE1 (pCDNA4/TO-IE1A) and HHV-6B IE1 (pCDNA4/TO-IE1B) control vector (pCDNA4/TO) were described previously (42). Plasmids expressing PML isoforms were kindly provided by Jin-Hyun Ahn (43). To generate a PML-I lentiviral vector, the PML-1 gene was PCR amplified with *attB1* and

attB2 sites added to the forward and reverse primer, respectively. The PCR amplicon was recombined into pDonor221 vector followed by a second recombination into pLenti CMV Hygro DEST vector, a kind gift from Eric Campeau and Paul Kaufman (Addgene plasmid # 17454) (44). The PML Double Nickase Plasmids (h2) (sc-400145-NIC-2) were bought from Santa Cruz Biotechnology (Santa Cruz, CA, USA).

Immunofluorescence (IFA)

Coverslips were incubated for 30 minutes in blocking solution (1 mg/ml BSA; 3% goat serum; 0.1% Triton X-100; 1 mM EDTA pH 8.0, in phosphate-buffered saline (PBS)). After blocking, coverslips were incubated for 1 hour in primary antibody diluted in blocking solution. Coverslips were washed with PBS, three times for five minutes. Coverslips were incubated for 30 minutes with secondary antibody diluted in blocking solution. Coverslips were washed with PBS, three times for five minutes. When the IFA was done, coverslips were air dried at room temperature and mounted with *SlowFade* Gold Antifade reagent containing DAPI (Invitrogen, Eugene, Oregon USA).

Immunofluorescence conjugated to *in situ* hybridization (IF-FISH)

Cells on coverslips were stained as for IFA. Once IFA was completed, cells were fixed for 2 minutes at room temperature with 1% paraformaldehyde in PBS. Coverslips were washed two times for five minutes with PBS. Cells were dehydrated with 5 minutes each consecutive ethanol baths (70%, 95%, 100%). Once dried, coverslips were placed upside down on a drop of hybridizing solution (70% formamide; 0.5% blocking reagent; 10 mM Tris-HCl pH 7.2; 1/1000 Cy3 or Cy5-TelC PNA probe). Samples were denatured for 10

163 minutes at 80°C on a heated block. Coverslips were incubated over night at 4°C in the dark
164 and washed two times for 15 minutes in washing solution (70% formamide; 10 mM Tris-
165 HCl pH 7.2). Coverslips were washed 3 time for 5 minutes with PBS and were air dried,
166 slow fade was added and coverslips were sealed.
167
168 **Transfection assays**
169 U2OS cells were seeded at 2 x 10^5 cells/well in a 6-well plate containing glass coverslips
170 in 2 mL of medium. Cells were transfected 24 hours post-seeding with pCDNA4/TO,
171 pCDNA4/TO-IE1A, pCDNA4/TO-IE1B expression vector using the *TransIT*-LT1
172 Transfection Reagent (Mirus Bio LLC, Madison, WI, USA). After 48 hours of transfection,
173 cells were washed 3 times with PBS and fixed in 2% of paraformaldehyde and used for
174 immunofluorescence (IFA) assay. HeLa LT cells were seeded at 1 x 10^5 cells/well in a 6-
175 well plate containing glass coverslips in 2 mL of medium. Cells were transfected 24 hours
176 post-seeding with pCDNA4/TO, pCDNA4/TO-IE1A, pCDNA4/TO-IE1B expression
177 vector using Lipofectamine 2000 (Thermo Fischer Scientific). After 48 hours of
178 transfection, cells were fixed in 2% paraformaldehyde and used for IFA.
179
180 **Infection assays**
181 U2OS cells were seeded at 2 x 10^5 cells/well in a 6-well plate containing glass coverslips
182 in 2 mL of medium. Cells were infected 24 hours post-seeding with U1102 (HHV-6A) and
183 Z29 (HHV-6B). After 48 hours post-infection, cells were washed 3 times with PBS and
184 fixed in 2% of paraformaldehyde and used for immunofluorescence (IFA) assay.
185

186 **Generation of PML Knockout cell line**

187 HeLa LT and U2OS cells were transfected with CRISPR-Cas9 vector targeting PML as
188 described. After 48 hours, cells were selected with 1 µg/mL of puromycin. Selected cells
189 were harvested, counted and seeded at a density of 1 cell per well in three 96-well flat-
190 bottom plates. After 10 to 14 days, wells containing only a single clone were identified.
191 Clones were propagated for an additional 3 weeks and transferred into wells of a 12-well
192 plate. Clones were screened by PCR, sequenced and analyzed by IFA for PML expression.
193 PML negative clones were expanded and kept frozen until used.

194

195 **HHV-6A/B integration assays**

196 Integration assays were performed as described previously (45). Briefly, ten thousand
197 cells per well (U2OS PML WT, U2OS PML$^{-/-}$ #1, U2OS PML$^{-/-}$ #2, HeLa LT PML
198 WT, HeLa LT PML$^{-/-}$ #1, HeLa LT PML$^{-/-}$ #2) were seeded in 48-well plates. The next
199 day, the cells were infected with U1102 or Z29 at a multiplicity of infection (MOI) of 1
200 followed by overnight incubation at 37°C. Cells were washed 3X with 1X PBS to remove
201 unabsorbed virions prior to the addition of fresh culture medium. Upon infection, cells
202 were passaged for 4 weeks and analyzed by droplet digital PCR (ddPCR). For this, DNA
203 was isolated using the QiaAMP blood extraction kit as described by the manufacturer
204 (Qiagen Inc., Toronto, ON, Canada).

205

206 **qPCR**

207 qPCR was performed as described previously by Gravel et al. (45). Briefly, DNA was
208 extracted using QiaAMP blood extraction kit as described by the manufacturer (Qiagen

Inc.) and analyzed using primers and probes against *U65-66* (HHV-6A/B) and *RPP30* (reference gene). Data was normalized against the corresponding genome copies of the cellular *RPP30* protein.

Quantification of HHV-6A/B integration by droplet digital PCR (ddPCR)

The HHV-6A/B copy number per cell was determined by ddPCR as previously described by Sedlak et al. (46).

Statistical analysis

Unpaired t-test with Welch correction was used to compare the number of PML-NBs at telomeres in IE1 expressing and control cells. It was also used to compare the number of IE1 at telomeres in $PML^{+/+}$ and $PML^{-/-}$ cells. Chi-square analysis was used to compare integration frequency between $PML^{+/+}$ and $PML^{-/-}$ cell lines.

Results

IE1A/B localize at the site of integration, the telomeres.

Upon cell entry, HHV-6A/B can either actively replicate or establish latency. This decision is often influenced by the permissivity of the target cells. We have previously shown that U2OS and Hela cells are semi-permissive to infection, as the HHV-6A/B initiates replication in only a minority of cells despite considerable expression of IE and E proteins (45), (47). Both cell lines have been extensively used to assess HHV-6A/B integration (48), (49), (50). To determine if IE proteins might contribute to HHV-6A/B integration, we first determined whether they localize to sites

232 of integration, the telomeres. U2OS cells were infected with HHV-6A (U1102) or
233 HHV-6B (Z29) for 2 days and analyzed for IE1 expression by confocal microscopy.
234 IE1 was detected as distinct nuclear foci upon infection (Fig 1A), with a proportion of
235 IE1 localizing with telomeres (yellow asterisks). Quantification of Z stacks revealed
236 that 20.4% and 26.38% of the IE1A/B foci (red) localize with telomeres (Fig 1B).
237 To assess if IE1A or IEB localize with cellular or viral telomeres, we transfected U2OS
238 cells with IE1A/B expression vectors and analyzed IE1 localization in the absence of
239 viral genomes. Ectopically-expressed IE1A and IE1B localized with cellular telomeres
240 to the same extent as during infection (Fig 2A and B), indicating that cellular telomeres
241 were targeted by these viral proteins.
242
243 **Both IE1A and IE1B colocalize with PML**
244 We previously demonstrated that IE1 of HHV-6B associates with PML-NBs during
245 productive T cell infection (31). We next determined IE1A and IE1B colocalization with
246 PML-NBs would also be observed in semi-permissive cells. IE1A and IE1B expression
247 vectors were transfected in U2OS cells and their localization was assessed by IFA. IE1
248 from both viruses efficiently associated with PML (Fig 3).
249 PML is actually not a single protein but a mixture of seven different isoforms, whereby
250 the first six isoforms (I to VI) are nuclear proteins (51). To determine if IE1
251 preferentially colocalizes with certain PML isoforms, we co-transfected PML negative
252 ($PML^{-/-}$) cells with individual expression plasmids for the six nuclear PML isoforms and
253 IE1 expression vectors. Western blotting confirmed that all six PML isoforms are
254 efficiently expressed upon transfection of $PML^{-/-}$ cells (Fig 4A). IE1B colocalized with

all PML isoform tested. Similarly, IE1A localized with all 6 PML isoforms (data not shown).

Presence of IE1A/B affects the number of PML-NBs present at cellular telomeres

U2OS cells do not express telomerase and elongate their telomeres via alternative lengthening of telomere mechanisms (ALT) (52), (41), (53). In ALT cells, a significant proportion (75%) of PML-NBs localize at telomeres and are referred to as ALT-associated PML-NBs (APBs) (Fig 5) (54). In Hela LT cells that rely mostly on the telomerase complex for telomere elongation the number of APBs was much lower (Fig 5).

Since IE1A/B colocalize with PML-NBs, we next assessed whether IE1's presence might affect PML-NBs localization at telomeres. U2OS and HeLa LT cells were transfected with IE1A/B expression vectors, and the proportion of PML-NBs localizing to telomeres was determined by IF-FISH (Fig 6A and B). The frequency of PML-NBs located at the host telomeres was reduced by 58% (25.8+/- 22.53) in U2OS cells upon expression of IE1A compared to the empty vector control (63.35+/- 16.97) (Fig 6C). A comparable reduction in APBs of 50% was also observed in U2OS cells expressing IE1B. We confirmed this observation in HeLa LT cells, where the PML-NBs localizing at telomeres was reduced by 64% and 61% upon expression ofIE1A and IE1B respectively. Similar results were obtained in U2OS and HeLa LT cells infected with HHV-6A/B (data not shown).

The absence of PML does not affect the presence of IE1A/B at telomeres.

Considering that IE1A/B colocalize with PML-NBs and that a significant proportion of PML-NBs are located at host telomeres, we next determined if PML contributes to the

278 localization of IE1A/B's to the telomeres. PML knockout (KO) U2OS and HeLa LT cell
279 were generated using the CRISPR-Cas9 system (Fig 7). Deletion of a part of exon 1 (Fig
280 7A) resulted in a pre-mature STOP codon resulting in a short truncated PML protein (Fig
281 7B). Abrogation of PML expression was confirmed in U2OS (Fig 7C) and HeLa LT (Fig
282 7D) cells by IFA.
283 Following transfection of IE1A/B expression vectors in WT and PML$^{-/-}$ U2OS cells, we
284 observed that IE1A/B localized at telomeres despite PML's absence, albeit at a slightly
285 lower frequency (Fig 8A and B). There was however an increased proportion of cells in
286 which IE1A/B were not present at telomeres. As shown in Fig 8C, the number of U2OS
287 PML$^{-/-}$ nuclei with no IE1A/B at telomeres was significantly increased relative to WT
288 nuclei (***$p<0.0001$).
289
290 **PML is required for efficient HHV-6A/B chromosomal integration.**
291 Considering that a proportion of PML-NBs localize at telomeres and that PML plays a role
292 in DNA repair by homologous recombination, we investigated if PML plays a role in HHV-
293 6A/B integration into telomeres. PML knockout and control cells lines were infected with
294 HHV-6A or HHV-6B and integration frequency assessed after four weeks post infection
295 by droplet digital PCR as described (48). The absence of PML was confirmed at the
296 beginning (T0) and the end (T28) of the experiment by IFA for U2OS (Fig 9A) and Hela
297 LT cells (Fig 10A). ddPCR revealed that HHV-6A and -6B integration was significantly
298 reduced in U2OS cells in the absence of PML by 64% and 50% respectively (Fig 9B and
299 C). In Hela LT cells, HHV-6A integration was reduced by approximately 50% in the
300 absence of PML (Fig 10B). The reductions were even more pronounced for HHV-6B in

HeLa LT cells where the integration frequency was reduced by 73% and 90.6% in the two independent clones used in this study (Fig 10C). Taken together, our data demonstrates that integration occurs less efficient in the absence of PML in two standard models for HHV-6A/B integration.

Discussion

One key interest of our laboratory is to identify proteins that facilitate HHV-6A/B chromosomal integration. We previously demonstrated that the putative HHV-6A/B integrase U94 possesses DNA binding, helicase and exonuclease activity, suggesting that the protein could be involved in HHV-6A/B integration (55). However, recombinant HHV-6A lacking U94 integrated as efficient as WT virus, indicating that U94 is dispensable for integration of HHV-6A in vitro (50).

Another hypothesis is that HHV-6A/B chromosomal integration occurs with the help of telomerase, the enzyme responsible for telomere elongation (56). We have previously shown that telomerase is not essential for HHV-6A/B integration, as it occurs in both telomerase negative and positive cells (48), (49). However, in telomerase expressing cells, telomerase is likely important for the generation a neo-telomere at the end of DR_L (reviewed in (57)). In support, blockade of telomerase activity by the G-quadruplex (guanine rich structure (G4) present in telomeres) stabilizing agent BRACO-19, negatively affects HHV-6A integration (49). Such effect is not observed in telomerase negative cells such as U2OS cells.

The fact that HHV-6A telomeric repeats are required for efficient integration (30) argues in favor of a homologous recombination (HR) events between cellular and viral telomeres. Cellular telomeres are protected by the shelterin complex that consists of 6 proteins: telomeric repeat binding factor 1 (TRF1), TRF2, protection of telomere 1 (POT1), telomere protection protein 1 (TPP1), TRF-interacting nuclear protein 2 (TIN2) and repressor activation protein 1 (RAP1) (58). The main function of the shelterin complex is to protect chromosome end from being recognized as damaged DNA. Of the 6 shelterin proteins, TRF2 is the key factor that blocks DNA repair proteins at telomeres by inhibiting the Ataxia-telangiectasia-mutated (ATM) pathway that senses double-stranded DNA breaks (59). In addition to the shelterin complex, other proteins can also localize to telomeres. In telomerase negative cells such as U2OS cells, telomeres are elongated by an Alternative Lengthening of Telomeres (ALT+) associated PML-Nuclear Bodies (APBs) mechanism (60),(54),(61),(62). These nuclear bodies primarily formed by the Promyelocytic Leukemia Protein (PML) itself that recruits hundreds of interacting partners at telomeres such as helicases implicated in G-quadruplex structure resolution like the bloom syndrome protein (BLM), the Werner Syndrome Protein (WRN) and other protein implicated in DNA recombination and repair (63), (54), (64), (65), (53). Osterwalds et al. have shown that in ALT^+ cells such as U2OS, PML-NBs (APBs) are frequently present at telomeres. We've confirmed this result (Fig 5). We also noticed that a significant proportion of PML-NBs also localize to telomeres of telomerase expressing cells such as HeLa LT cell (Fig 5), in agreement with Marchesini et al (63). Marchesini demonstrated that PML is essential for telomere maintenance in non-neoplastic cells, as cells undergo apoptosis in absence of PML after DNA damage at these sites (63). These findings support the role of PML in

347 DNA repair mechanism. Considering this, we hypothesized that PML could aid in HHV-
348 6A/B integration.
349
350 In addition to their roles in telomere stability, PML-NBs have antiviral defense functions
351 (36), (35). In contrast to many other viruses including HSV, CMV, EBV and HHV-8,
352 HHV-6A/B infection does not lead to the dispersal of PML-NBs but rather to PML-NBs
353 coalescence (38), (66), (67), (68), (33). Whether this affects antiviral functions of PML-
354 NBs remains to be determined. We could demonstrate that the HHV-6A/B IE1 protein, a
355 protein that play roles in innate immune evasion mechanisms (69), (42), is associated with
356 PML-NBs (31). Here we also report that IE1A/B also associates with telomeres.
357 Considering that PML also associates with telomeres, we hypothesized that IE1A/B
358 localization to telomeres could be PML dependent. However, in PML$^{-/-}$ U2OS and HeLa
359 LT cells, a significant proportion of IE1A/B remained associated with telomeres. However,
360 the proportion of nuclei in which IE1A/B could not be detected at telomeres was largely
361 increased in PML$^{-/-}$ cells. Thus, although not essential, PML does influence the
362 localization of IE1A/B at telomeres. One possible explanation resides in the fact that
363 IE1A/B are SUMOylated proteins and that PML itself and/or other PML-NB associated
364 proteins contain SUMO interacting motif (SIM) could facilitate interactions at telomeres
365 (31), (70). Moreover, IE1A/B also possess putative SIMs that can bind SUMOylated
366 proteins present at telomeres, possibly explaining why IE1A/B can localize at telomeres in
367 the absence of PML.
368

Finally, we tested if PML played a role in HHV-6A/B chromosomal integration. We used the CRISPR-Cas9 to abrogate PML expression (Fig 7). For each cell line used, two independent PML KO clones were assessed to ensure reproducibility and avoid potential off-target effects. In U2OS cells (Fig 9), HHV-6B integration was less frequent in $PML^{-/-}$ cells ($p<0.0001$). In HeLa LT cells (Fig 10), the same effect was observed for HHV-6A and HHV-6B. Of note, integration rates are higher in U2OS presumably because of higher constitutive DDR repair in the cells, supporting the hypothesis that DNA repair mechanisms are involved in the HHV-6A/B integration process (71). Globally, both cell lines studied suggest a role for PML in HHV-6A/B integration. However, since integration still occurred in PML KO cells indicates that PML contributes but is not essential for this process. The positive influence of PML on HHV-6A/B integration could be explained by a reduction of protein present at telomeres like those involve in the DDR. As mentioned above, TRF2 blocks DNA repair at double DNA strand breaks. Moreover, in PML-NBs at telomeres, TRF2 is SUMOylated by MMS21, resulting in a lower density of TRF2 on telomeres (72). These telomere regions can then be processed by other proteins and recombine with the HHV-6A/B telomeres.

In conclusion, we have demonstrated that HHV-6A/B IE1 proteins colocalize with all isoforms of PML and host telomeres. Abrogation of PML expression influences the presence of IE1 at telomeres and affects HHV-6A/B integration into host telomeres. To our knowledge, this is the first report of a cellular protein that is involved in HHV-6A/B integration.

References

1. Ablashi D, Agut H, Alvarez-Lafuente R, Clark DA, Dewhurst S, DiLuca D, et al. Classification of HHV-6A and HHV-6B as distinct viruses. Arch Virol [Internet]. 2014;159(5):863–70. Available from: http://dx.doi.org/10.1007/s00705-013-1902-5

2. Yamanishi K, Shiraki K, Kondo T, Okuno T, Takahashi M, Asano Y, et al. Identification of Human Herpesvirus-6 as a Causal Agent for Exhentem Subitum. Lancet [Internet]. 1988;331(8594):1065–7. Available from: http://www.sciencedirect.com/science/article/pii/S0140673688918934

3. Ballestas ME, Chatis PA, Kaye KM. Efficient persistence of extrachromosomal KSHV DNA mediated by latency- associated nuclear antigen. Science (80-) [Internet]. 1999;284(5414):641–4. Available from: http://www.ncbi.nlm.nih.gov/cgi-bin/Entrez/referer?http://www.sciencemag.org/cgi/content/full/284/5414/641

4. Marechal V, Dehee A, Chikhi-Brachet R, Piolot T, Coppey-Moisan M, Nicolas JC. Mapping EBNA-1 domains involved in binding to metaphase chromosomes. J Virol. 1999;73(5):4385–92.

5. Quintela A, Escuret V, Roux S, Bonnafous P, Gilis L, Barraco F, et al. HHV-6 infection after allogeneic hematopoietic stem cell transplantation: From chromosomal integration to viral co-infections and T-cell reconstitution patterns. J Infect. 2016;72(2):214–22.

6. Sedlak RH, Hill JA, Nguyen T, Cho M, Levin G, Cook L, et al. Detection of

human herpesvirus 6B (HHV-6B) reactivation in hematopoietic cell transplant recipients with inherited chromosomally integrated HHV-6A by droplet digital PCR. J Clin Microbiol. 2016;54(5):1223–7.

7. Miura H, Kawamura Y, Hattori F, Tanaka M, Kudo K, Ihira M, et al. Late-phase human herpesvirus 6B reactivation in hematopoietic stem cell transplant recipients. Transpl Infect Dis [Internet]. 2018;(May):e12916. Available from: http://doi.wiley.com/10.1111/tid.12916

8. Sang Y, Zhang R, Scott WRP, Creagh AL, Haynes CA, Straus SK. U24 from Roseolovirus interacts strongly with Nedd4 WW Domains. Sci Rep [Internet]. 2017;7(November 2016):1–11. Available from: http://dx.doi.org/10.1038/srep39776

9. Campbell A, Hogestyn JM, Folts CJ, Lopez B, Pröschel C, Mock D, et al. Expression of the Human Herpesvirus 6A Latency-Associated Transcript U94A Disrupts Human Oligodendrocyte Progenitor Migration. Sci Rep. 2017;7(1):1–7.

10. Eimer WA, Vijaya Kumar DK, Navalpur Shanmugam NK, Rodriguez AS, Mitchell T, Washicosky KJ, et al. Alzheimer's Disease-Associated β-Amyloid Is Rapidly Seeded by Herpesviridae to Protect against Brain Infection. Neuron. 2018;56–63.

11. Readhead B, Haure-Mirande JV, Funk CC, Richards MA, Shannon P, Haroutunian V, et al. Multiscale Analysis of Independent Alzheimer's Cohorts Finds Disruption of Molecular, Genetic, and Clinical Networks by Human Herpesvirus. Neuron [Internet]. 2018;99(1):64–82.e7. Available from: https://doi.org/10.1016/j.neuron.2018.05.023

438 12. Daibata M, Taguchi T, Nemoto Y, Taguchi H, Miyoshi I. Inheritance of
439 chromosomally integrated human herpesvirus 6 DNA. Blood. 1999;94:1545–9.
440 13. Luppi M, Marasca R, Barozzi P, Ferrari S, Ceccherini-Nelli L, Batoni G, et al.
441 Three cases of human herpesvirus-6 latent infection: integration of viral genome in
442 peripheral blood mononuclear cell DNA. J Med Virol [Internet]. 1993;40(1):44–
443 52. Available from: http://www.ncbi.nlm.nih.gov/pubmed/8099945
444 14. Potenza L, Barozzi P, Masetti M, Pecorari M, Bresciani P, Gautheret-Dejean a, et
445 al. Prevalence of human herpesvirus-6 chromosomal integration (CIHHV-6) in
446 Italian solid organ and allogeneic stem cell transplant patients. Am J Transplant
447 [Internet]. 2009;9(7):1690–7. Available from:
448 http://www.ncbi.nlm.nih.gov/pubmed/19519818
449 15. Miura H, Kawamura Y, Kudo K, Ihira M, Ohye T, Kurahashi H, et al. Virological
450 analysis of inherited chromosomally integrated human herpesvirus-6 in three
451 hematopoietic stem cell transplant patients. Transpl Infect Dis. 2015;17(5):728–31.
452 16. Tanaka-Taya K, Sashihara J, Kurahashi H, Amo K, Miyagawa H, Kondo K, et al.
453 Human herpesvirus 6 (HHV-6) is transmitted from parent to child in an integrated
454 form and characterization of cases with chromosomally integrated HHV-6 DNA. J
455 Med Virol. 2004;73(3):465–73.
456 17. Zhang E, Bell AJ, Wilkie GS, Suárez NM, Batini C, Veal CD, et al. Inherited
457 Chromosomally Integrated Human Herpesvirus 6 Genomes Are Ancient, Intact,
458 and Potentially Able To Reactivate from Telomeres. J Virol. 2017;91(22):1–19.
459 18. Politikos I, Mcmasters M, Bryke C, Avigan D, Boussiotis VA. Possible
460 reactivation of chromosomally integrated human herpesvirus 6 after treatment with

461 histone deacetylase inhibitor. 2018;2(12):1367–70.

462 19. Endo A, Watanabe K, Ohye T, Suzuki K, Matsubara T, Shimizu N, et al.
463 Molecular and virological evidence of viral activation from chromosomally
464 integrated human herpesvirus 6A in a patient with X-linked severe combined
465 immunodeficiency. Clin Infect Dis. 2014;59(4):545–8.

466 20. Strenger V, Caselli E, Lautenschlager I, Schwinger W, Aberle SW, Loginov R, et
467 al. Detection of HHV-6-specific mRNA and antigens in PBMCs of individuals
468 with chromosomally integrated HHV-6 (ciHHV-6). Clin Microbiol Infect
469 [Internet]. 2014;20(10):1027–32. Available from: http://dx.doi.org/10.1111/1469-
470 0691.12639

471 21. Zhang E, Cotton VE, Hidalgo-bravo A, Huang Y, Bell AJ, Jarrett RF, et al. HHV-
472 8-unrelated primary effusion- like lymphoma associated with clonal loss of
473 inherited herpesvirus-6A from the telomere of chromosome 19q.
474 2016;(February):2–10.

475 22. Griffith JD, Comeau L, Rosenfield S, Stansel RM, Bianchi A, Moss H, et al.
476 Mammalian Telomeres End in a Large Duplex Loop. Cell [Internet].
477 1999;97(4):503–14. Available from:
478 http://www.sciencedirect.com/science/article/pii/S0092867400807606

479 23. de Lange T. How telomeres solve the end-protection problem. Science (80-)
480 [Internet]. 2009;326(5955):948–52. Available from:
481 http://www.ncbi.nlm.nih.gov/pubmed/19965504

482 24. van Steensel B, Smogorzewska A, de Lange T. TRF2 Protects Human Telomeres
483 from End-to-End Fusions. Cell [Internet]. 1998;92(3):401–13. Available from:

http://www.sciencedirect.com/science/article/pii/S0092867400809320

25. Sfeir A, de Lange T. Removal of Shelterin Reveals the Telomere End-Protection Problem. Science (80-) [Internet]. 2012;336(6081):593–7. Available from: http://science.sciencemag.org/content/336/6081/593

26. Isegawa Y, Mukai T, Nakano K, Kagawa M, Chen J, Mori Y, et al. Comparison of the complete DNA sequences of human herpesvirus 6 variants A and B. J Virol [Internet]. 1999;73(10):8053–63. Available from: http://www.ncbi.nlm.nih.gov/pubmed/10482554%0Ahttp://www.pubmedcentral.nih.gov/articlerender.fcgi?artid=PMC112821

27. Dominguez G, Dambaugh TR, Stamey FR, Dewhurst S, Inoue N, Pellett PE. Human herpesvirus 6B genome sequence: coding content and comparison with human herpesvirus 6A. J Virol. 1999;73(10):8040–52.

28. Martin ME, Nicholas J, Thomson BJ, Newman C, Honess RW. Identification of a transactivating function mapping to the putative immediate-early locus of human herpesvirus 6. J Virol [Internet]. 1991;65(10):5381–90. Available from: http://www.pubmedcentral.nih.gov/articlerender.fcgi?artid=249019&tool=pmcentrez&rendertype=abstract

29. Gompels UA, Macaulay HA. Characterization of Human Telomeric Repeat Sequences from Human Herpesvirus-6 and Relationship to Replication. J Gen Virol. 1995;76(1995):451–8.

30. Wallaschek N, Sanyal A, Pirzer F, Gravel A, Mori Y, Flamand L, et al. The Telomeric Repeats of Human Herpesvirus 6A (HHV-6A) Are Required for Efficient Virus Integration. PLoS Pathog. 2016;12(5):1–15.

507 31. Gravel A, Gosselin J, Flamand L. Human herpesvirus 6 immediate-early 1 protein
508 is a sumoylated nuclear phosphoprotein colocalizing with promyelocytic leukemia
509 protein-associated nuclear bodies. J Biol Chem. 2002;277(22):19679–87.
510 32. Gravel A, Dion V, Cloutier N, Gosselin J, Flamand L. Characterization of human
511 herpesvirus 6 variant B immediate-early 1 protein modifications by small
512 ubiquitin-related modifiers. J Gen Virol. 2004;85(5):1319–28.
513 33. Stanton R, Fox JD, Caswell R, Sherratt E, Wilkinson GW. Analysis of the human
514 herpesvirus-6 immediate-early 1 protein. J Gen Virol [Internet]. 2002;83(Pt
515 11):2811–20. Available from: http://www.ncbi.nlm.nih.gov/pubmed/12388818
516 34. Chen D, Feng C, Tian X, Zheng N, Wu Z. PML restricts enterovirus 71 replication
517 by inhibiting autophagy. Front Immunol [Internet]. 2018;9(June):1268. Available
518 from: https://www.frontiersin.org/articles/10.3389/fimmu.2018.01268/abstract
519 35. Scherer M, Stamminger T. Emerging Role of PML Nuclear Bodies in Innate
520 Immune Signaling. 2016;90(13):5850–4.
521 36. Xu P, Roizman B. The SP100 component of ND10 enhances accumulation of
522 PML and suppresses replication and the assembly of HSV replication
523 compartments. Proc Natl Acad Sci [Internet]. 2017;201703395. Available from:
524 http://www.pnas.org/lookup/doi/10.1073/pnas.1703395114
525 37. Xu P, Mallon S, Roizman B. PML plays both inimical and beneficial roles in
526 HSV-1 replication. Proc Natl Acad Sci [Internet]. 2016;113(21):E3022–8.
527 Available from: http://www.pnas.org/lookup/doi/10.1073/pnas.1605513113
528 38. Wang S, Long J, Zheng C fu. The potential link between PML NBs and ICP0 in
529 regulating lytic and latent infection of HSV-1. Protein Cell. 2012;3(5):372–82.

530 39. Ishov AM, Stenberg RM, Maul GG. Human cytomegalovirus immediate early
531 interaction with host nuclear structures: Definition of an immediate transcript
532 environment. J Cell Biol. 1997;138(1):5–16.
533 40. Sanyal A, Wallaschek N, Glass M, Flamand L, Wight D, Kaufer B. The ND10
534 Complex Represses Lytic Human Herpesvirus 6A Replication and Promotes
535 Silencing of the Viral Genome. Viruses [Internet]. 2018;10(8):401. Available
536 from: http://www.mdpi.com/1999-4915/10/8/401
537 41. Roderick J. O'Sullivan, Nausica Arnoult, Daniel H. Lackner, Liana Oganesian,
538 Candy Haggblom, Armelle Corpet, Genevieve Almouzni and JK. Rapid induction
539 of Alternative Lengthening of Telomeres by depletion of the histone chaperone
540 ASF1. 2014;21(2):167–74.
541 42. Jaworska J, Gravel A, Fink K, Grandvaux N, Flamand L. Inhibition of
542 Transcription of the Beta Interferon Gene by the Human Herpesvirus 6 Immediate-
543 Early 1 Protein. J Virol [Internet]. 2007;81(11):5737–48. Available from:
544 http://jvi.asm.org/cgi/doi/10.1128/JVI.02443-06
545 43. Kim Y-E, Ahn J-H. Positive role of promyelocytic leukemia protein in type I
546 interferon response and its regulation by human cytomegalovirus. PLoS Pathog
547 [Internet]. 2015;11(3):e1004785. Available from:
548 http://journals.plos.org/plospathogens/article?id=10.1371/journal.ppat.1004785
549 44. Campeau E, Ruhl VE, Rodier F, Smith CL, Rahmberg BL, Fuss JO, et al. A
550 versatile viral system for expression and depletion of proteins in mammalian cells.
551 PLoS One. 2009;4(8).
552 45. Gravel A, Dubuc I, Wallaschek N, Gilbert-Girard S, Collin V, Hall-Sedlak R, et al.

553 Cell culture systems to study Human Herpesvirus 6A/B Chromosomal Integration.
554 J Virol [Internet]. 2017;(May):JVI.00437-17. Available from:
555 http://jvi.asm.org/lookup/doi/10.1128/JVI.00437-17
556 46. Sedlak RH, Cook L, Huang ML, Magaret A, Zerr DM, Boeckh M, et al.
557 Identification of chromosomally integrated human herpesvirus 6 by droplet digital
558 PCR. Clin Chem. 2014;60(5):765–72.
559 47. Worrad DM, Caradonna S. Identification of the coding sequence for herpes
560 simplex virus uracil-DNA glycosylase. J Virol [Internet]. 1988;62(12):4774–7.
561 Available from:
562 http://www.ncbi.nlm.nih.gov/entrez/query.fcgi?cmd=Retrieve&db=PubMed&dopt
563 =Citation&list_uids=2846888
564 48. Gravel A, Dubuc I, Wallaschek N, Gilbert-Girard S, Collin V, Hall-Sedlak R, et al.
565 Cell Culture Systems To Study Human Herpesvirus 6A/B Chromosomal
566 Integration. J Virol [Internet]. 2017;91(14):e00437-17. Available from:
567 http://jvi.asm.org/lookup/doi/10.1128/JVI.00437-17
568 49. Gilbert-Girard S, Gravel A, Artusi S, Richter SN, Wallaschek N, Kaufer BB, et al.
569 Stabilization of telomere G-quadruplexes interferes with human herpesvirus 6A
570 chromosomal integration. J Virol [Internet]. 2017;(May):JVI.00402-17. Available
571 from: http://jvi.asm.org/lookup/doi/10.1128/JVI.00402-17
572 50. Wallaschek N, Gravel A, Flamand L, Kaufer BB. The putative U94 integrase is
573 dispensable for human herpesvirus 6 (HHV-6) chromosomal integration. J Gen
574 Virol. 2016;97(8):1899–903.
575 51. Maroui MA, Maarifi G, Mc Manus FP, Lamoliatte F, Thibault P, Chelbi-Alix MK.

576 Promyelocytic Leukemia Protein (PML) Requirement for Interferon-induced
577 Global Cellular SUMOylation. Mol Cell Proteomics. 2018;17(6):1196–208.
578 52. Bryan TM, Englezou A, Gupta J, Bacchetti S, Reddel RR. Telomere elongation in
579 immortal human cells without detectable telomerase activity. Embo J [Internet].
580 1995;14(17):4240–8. Available from:
581 http://www.ncbi.nlm.nih.gov/pmc/articles/PMC394507/pdf/emboj00041-0128.pdf
582 53. Jiang WQ, Zhong ZH, Nguyen A, Henson JD, Toouli CD, Braithwaite AW, et al.
583 Induction of alternative lengthening of telomeres-associated PML bodies by
584 p53/p21 requires HP1 proteins. J Cell Biol. 2009;185(5):797–810.
585 54. Osterwald S, Deeg KI, Chung I, Parisotto D, Worz S, Rohr K, et al. PML induces
586 compaction, TRF2 depletion and DNA damage signaling at telomeres and
587 promotes their alternative lengthening. J Cell Sci [Internet]. 2015;128(10):1887–
588 900. Available from: http://jcs.biologists.org/cgi/doi/10.1242/jcs.148296
589 55. Trempe F, Gravel A, Dubuc I, Wallaschek N, Collin V, Gilbert-Girard S, et al.
590 Characterization of human herpesvirus 6A/B U94 as ATPase, helicase,
591 exonuclease and DNA-binding proteins. Nucleic Acids Res [Internet].
592 2015;43(12):6084–98. Available from:
593 http://nar.oxfordjournals.org/lookup/doi/10.1093/nar/gkv503
594 56. Sauerwald A, Sandin S, Cristofari G, Scheres SHW, Lingner J, Rhodes D.
595 Structure of active dimeric human telomerase. Nat Struct Mol Biol [Internet]. 2013
596 Apr;20(4):454–60. Available from: http://dx.doi.org/10.1038/nsmb.2530
597 57. Collin V, Flamand L. HHV-6A/B Integration and the Pathogenesis Associated
598 with the Reactivation of Chromosomally Integrated HHV-6A/B. Viruses

599 [Internet]. 2017;9(7):160. Available from: http://www.mdpi.com/1999-
600 4915/9/7/160
601 58. Palm W, de Lange T. How Shelterin Protects Mammalian Telomeres. Annu Rev
602 Genet [Internet]. 2008;42(1):301–34. Available from:
603 http://dx.doi.org/10.1146/annurev.genet.41.110306.130350
604 59. Denchi EL, de Lange T. Protection of telomeres through independent control of
605 ATM and ATR by TRF2 and POT1. Nature [Internet]. 2007 Aug
606 30;448(7157):1068–71. Available from: http://dx.doi.org/10.1038/nature06065
607 60. Chang HR, Munkhjargal A, Kim M-J, Park SY, Jung E, Ryu J-H, et al. The
608 functional roles of PML nuclear bodies in genome maintenance. Mutat Res Mol
609 Mech Mutagen [Internet]. 2017;(May):0–1. Available from:
610 http://www.sciencedirect.com/science/article/pii/S0027510717300404
611 61. Osterrieder N, Wallaschek N, Kaufer BB. Herpesvirus Genome Integration into
612 Telomeric Repeats of Host Cell Chromosomes. Annu Rev Virol [Internet].
613 2014;1(1):215–35. Available from:
614 http://www.annualreviews.org/doi/full/10.1146/annurev-virology-031413-085422
615 62. Yeager TR, Neumann A a, Englezou A, Leukemia P, Body PML, Huschtscha LI,
616 et al. Telomerase-negative Immortalized Human Cells Contain a Novel Type of
617 Promyelocytic Leukemia (PML) Body Advances in Brief Telomerase-negative
618 Immortalized Human Cells Contain a Novel Type of. 1999;4175–9.
619 63. Marchesini M, Matocci R, Tasselli L, Cambiaghi V, Orleth A, Furia L, et al. PML
620 is required for telomere stability in non-neoplastic human cells. Oncogene
621 [Internet]. 2016;35(14):1811–21. Available from:

622 http://www.nature.com/doifinder/10.1038/onc.2015.246

623 64. Shamanna RA, Lu H, de Freitas JK, Tian J, Croteau DL, Bohr VA. WRN regulates
624 pathway choice between classical and alternative non-homologous end joining.
625 Nat Commun [Internet]. 2016;7(May):13785. Available from:
626 http://www.nature.com/doifinder/10.1038/ncomms13785

627 65. Tikoo S, Madhavan V, Hussain M, Miller ES, Arora P, Zlatanou A, et al.
628 Ubiquitin-dependent recruitment of the Bloom Syndrome helicase upon replication
629 stress is required to suppress homologous recombination. EMBO J [Internet].
630 2013;32(12):1778–92. Available from: http://dx.doi.org/10.1038/emboj.2013.117

631 66. Marcos-Villar L, Lopitz-Otsoa F, Gallego P, Muñoz-Fontela C, González-
632 Santamaría J, Campagna M, et al. Kaposi's sarcoma-associated herpesvirus protein
633 LANA2 disrupts PML oncogenic domains and inhibits PML-mediated
634 transcriptional repression of the survivin gene. J Virol [Internet].
635 2009;83(17):8849–58. Available from:
636 http://www.pubmedcentral.nih.gov/articlerender.fcgi?artid=2738140&tool=pmcen
637 trez&rendertype=abstract

638 67. Eva-Maria Schilling, Myriam Scherer, Nina Reuter, Johannes Schweininger, Yves
639 A. Muller TS. The Human Cytomegalovirus IE1 Protein Antagonizes PML
640 Nuclear Body- Mediated Intrinsic Immunity via the Inhibition of PML De Novo
641 SUMOylation. J Virol. 2017;91(4):1–17.

642 68. Sivachandran N, Wang X, Frappier L. Functions of the Epstein-Barr Virus EBNA1
643 Protein in Viral Reactivation and Lytic Infection. J Virol [Internet].
644 2012;86(11):6146–58. Available from:

645 http://jvi.asm.org/cgi/doi/10.1128/JVI.00013-12

646 69. Jaworska J, Gravel A, Flamand L. Divergent susceptibilities of human herpesvirus
647 6 variants to type I interferons. Proc Natl Acad Sci U S A [Internet].
648 2010;107(18):8369–74. Available from:
649 http://www.pubmedcentral.nih.gov/articlerender.fcgi?artid=2889514&tool=pmcen
650 trez&rendertype=abstract

651 70. Chang HR, Munkhjargal A, Kim MJ, Park SY, Jung E, Ryu JH, et al. The
652 functional roles of PML nuclear bodies in genome maintenance. Mutat Res -
653 Fundam Mol Mech Mutagen [Internet]. 2018;809(April 2017):99–107. Available
654 from: https://doi.org/10.1016/j.mrfmmm.2017.05.002

655 71. Dunham M a, Neumann A a, Fasching CL, Reddel RR. Telomere maintenance by
656 recombination in human cells. Nat Genet [Internet]. 2000;26(4):447–50. Available
657 from:
658 http://www.ncbi.nlm.nih.gov/entrez/query.fcgi?db=pubmed&cmd=Retrieve&dopt
659 =AbstractPlus&list_uids=11101843

660 72. Walker JR, Zhu XD. Post-translational modifications of TRF1 and TRF2 and their
661 roles in telomere maintenance. Mech Ageing Dev [Internet]. 2012;133(6):421–34.
662 Available from: http://dx.doi.org/10.1016/j.mad.2012.05.002

663

664 # Figures

665

666 **Fig 1. Colocalization of IE1A/B at telomeres in infection.** U2OS cells were infected
667 with U1102 (HHV-6A) and Z29 (HHV-6B). A) 48 hours post-infection, cells were fixed

668 with 2% paraformaldehyde and labeled for IF-FISH. IE1A/B was detected using anti-IE1-
669 ALEXA-568 (red) labeled antibodies and telomeres were detected using a Cy5-labeled
670 telomeric probe (Aqua). B) Percentage of IE1A/B foci localizing at telomeres in infected
671 cells. P value was determined using an unpaired t-test with Welch correction. ns: p value
672 is not significant.
673
674 **Fig 2. Colocalization of IE1A/B at telomeres in transfection.** (A) U2OS cells were
675 transfected with pCDNA4TO (CTRL) and pCDNA4TO-IE1A/B expression vectors. Cells
676 were analyzed by immunofluorescence (IFA) 48 hours post-transfection, using anti-IE1
677 ALEXA-568-labeled (red) and anti-PML ALEXA-488-labeled antibodies (green). (B)
678 Percentage of IE1A/B foci localizing at telomeres in transfected cells. P value was
679 determined using an unpaired t-test with Welch correction. *P<0.04.
680
681 **Fig 3. Ectopic IE1A/B colocalize with PML.** U2OS were transfected with IE1A/B
682 expression vectors. 48 hours post-transfection, cells were analyzed by IFA using anti-PML
683 ALEXA-488-labeled (green) and anti-IE1 ALEXA-568-labeled (red) antibodies.
684
685 **Fig 4. IE1A/B colocalize with all nuclear PML isoforms.** (A) HEK293T were
686 transfected with PML isoforms expression vectors and analyzed by western blot using anti-
687 Myc antibodies. U2OS $PML^{-/-}$ were co-transfected using pCDNA4TO-IE1B (B) vectors
688 along with vectors expressing the various PML isoforms (I to VI). 48 hours post-
689 transfection, cells were analyzed by IFA using anti-Myc ALEXA-488-labeled (green) and
690 anti-IE1 ALEXA-568-labeled (red) antibodies.

691

692 **Fig 5. PML proteins colocalize at telomeres in U2OS and HeLa LT cells.** (A) U2OS
693 cells (ALT+) and HeLa LT cells (telomerase +) were grown on coverslips and fixed with
694 2% paraformaldehyde at sub confluence. Cells were analyzed by IF-FISH. PML proteins
695 were detected using anti-PML ALEXA-488-labeled (green) antibodies and telomeres were
696 detected using a Cy3-labeled telomeric probe (red). (B) The number of PML foci localizing
697 at telomeres was calculated after analysis of U2OS (N=20) and HeLa LT (N=40) nuclei.

698

699 **Fig 6. IE1A/B colocalize with PML at telomeres.** U2OS (A) and HeLa LT (B) cells were
700 transfected with pCDNA4/TO-IE1A or pCDNA4/TO-IE1B. 48 hours post-transfection,
701 cells were fixed with 2% paraformaldehyde and analyzed by IF-FISH. IE1A/B were
702 detected using anti-IE1-ALEXA-568-labeled antibodies (red), PML were detected using
703 anti-PML ALEXA-488-labeled (green) antibodies and telomeres were labeled using a Cy5-
704 labeled telomeric probe (Aqua). (C) Percentage of IE1A/B at telomeres in transfected
705 U2OS (N=37) and HeLa LT (N=24) cells. P value was determined using an unpaired t-test
706 with Welch correction. *P<0.01; ns = p value is not significant. (D) Percentage of PML
707 foci at telomeres in presence and in absence of ectopically expressed IE1A/B. CTRL:
708 Empty vector. P value was determined using an unpaired t-test with Welch correction.
709 ***p<0.0001

710

711 **Fig 7. Generation of PML Knockout cell lines.** U2OS and HeLa LT cells were
712 transfected with expression vectors for Cas-9 nuclease and PML RNA guides. After
713 puromycin selection, cells were seeded at a density of one cell/well to obtain unique clones.

(A) Each clone was screened by PCR with PML primers. Mutations were confirmed by sequencing the PCR amplicons. (B) Translation of the mutated sequence results into a truncated protein with three premature STOP codons. WT and PML$^{-/-}$ U2OS (C) and HeLa LT (D) cells were analyzed by IFA for PML expression using anti-PML ALEXA-488-labeled (green) antibodies.

Fig 8. PML is dispensable for IE1A/B localization at telomeres (A) U2OS$^{-/-}$ cells were transfected with pCDNA4TO-IE1A and pCDNA4TO-IE1B expression vectors. 48 hours post-transfection, cells were analyzed by IF-FISH for IE1A/B (red) and PML (green) expression using specific antibodies. Telomeres were detected using Cy5-labeled telomeric probe (Aqua). (B) Number of IE1A/B foci localizing at telomeres in the presence (N=37 for IE1A PML$^{+/+}$; N=24 for IE1B PML$^{+/+}$) or in the absence of PML (N=46 for IE1A PML$^{-/-}$; N=35 for IE1B PML$^{-/-}$). P value was determined using an unpaired t-test with Welch correction. *P<0.01. ns: p value is not significant. (C) Total number of IE1A/B that have no IE1A/B at telomeres was compared between PML$^{+/+}$ (N=37 for IE1A; N=24 for IE1B) and $^{-/-}$ cell lines (N=46 for IE1A; N=35 for IE1B). P value was determined using Chi-square analysis. ***P<0.0001

Fig 9. HHV-6A/B integration in WT and PML $^{-/-}$ U2OS cells. (A) PML expression in WT and PML$^{-/-}$ U2OS cells on day 0 and day 28 post-infection. WT and PML$^{-/-}$ U2OS cells were infected at a MOI of 1 with HHV-6A (B) and HHV-6B (C) and were cultured for a month. Cellular DNA was extracted, and integration frequency determined by ddPCR. Each integration assay was done three time for each cell lines (error bars). CTRL + :

737 iciHHV-6A/B donor DNA. P value was determined using Chi-square analysis. P value was
738 determined using Chi-square analysis. ***P<0.0001; **P<0.001
739
740 **Fig 10. HHV-6A/B integration in WT and PML $^{-/-}$ HeLa LT cells.** (A) PML expression
741 in WT and PML$^{-/-}$ HeLa LT cells on day 0 and day 28 post-infection. WT and PML$^{-/-}$
742 HeLa LT cells were infected at a MOI of 1 with HHV-6A (B) and HHV-6B (C) and were
743 cultured for a month. Cellular DNA was extracted, and integration frequency determined
744 by ddPCR. Each integration assay was done three time for each cell lines (error bars).
745 CTRL + : iciHHV-6A/B donor DNA. P value was determined using Chi-square analysis.
746 ***P<0.0001; ns: p value is not significant.
747

748 Supporting information

749
750 **S1 Fig. PML KO does not create more DNA damages.** PML$^{+/+}$ and PML$^{-/-}$ cells from
751 the integration assays at T28 were seeded on coverslips and fixed with 2% of
752 paraformaldehyde. Cells were analyzed by IF-FISH for DNA damage protein 53BP1 (red)
753 and PML (green) expression using specific antibodies. Telomeres and nuclei were detected
754 using Cy5-labeled telomeric probe (Aqua). Number of 53BP1 foci per nuclei was counted
755 for PML$^{+/+}$ U2OS cells (N=42), HeLa LT cells (N=37) and PML$^{-/-}$ U2OS cells (N=40)
756 and HeLa LT cells (N=37). P value was determined using an unpaired t-test with Welch
757 correction. ns: p value is not significant.
758

759 **S2. PML and IE1B localize in close proximity.** U2OS-Flp-In TREX cells were
760 transfected with expression vectors containing FLAG-BirA-GFP and FLAG-BirA-IE1B
761 and selected with hygromycin (250µg/ml) and blasticidin (50µg/ml). (B) Cells were seeded
762 on coverslips and 24 hours later, 50nM of biotin was added to the medium for an additional
763 24h before being fixed with paraformaldehyde 2%. IFA confirms BirA-GFP and BirA-
764 IE1B expression (Flag) and biotinylation of proteins (Streptavidin-HRP). (C) Biotinylated
765 proteins were immunoprecipitated with streptavidin magnetic beads followed by mass
766 spectrometry.
767
768
769
770

(A)

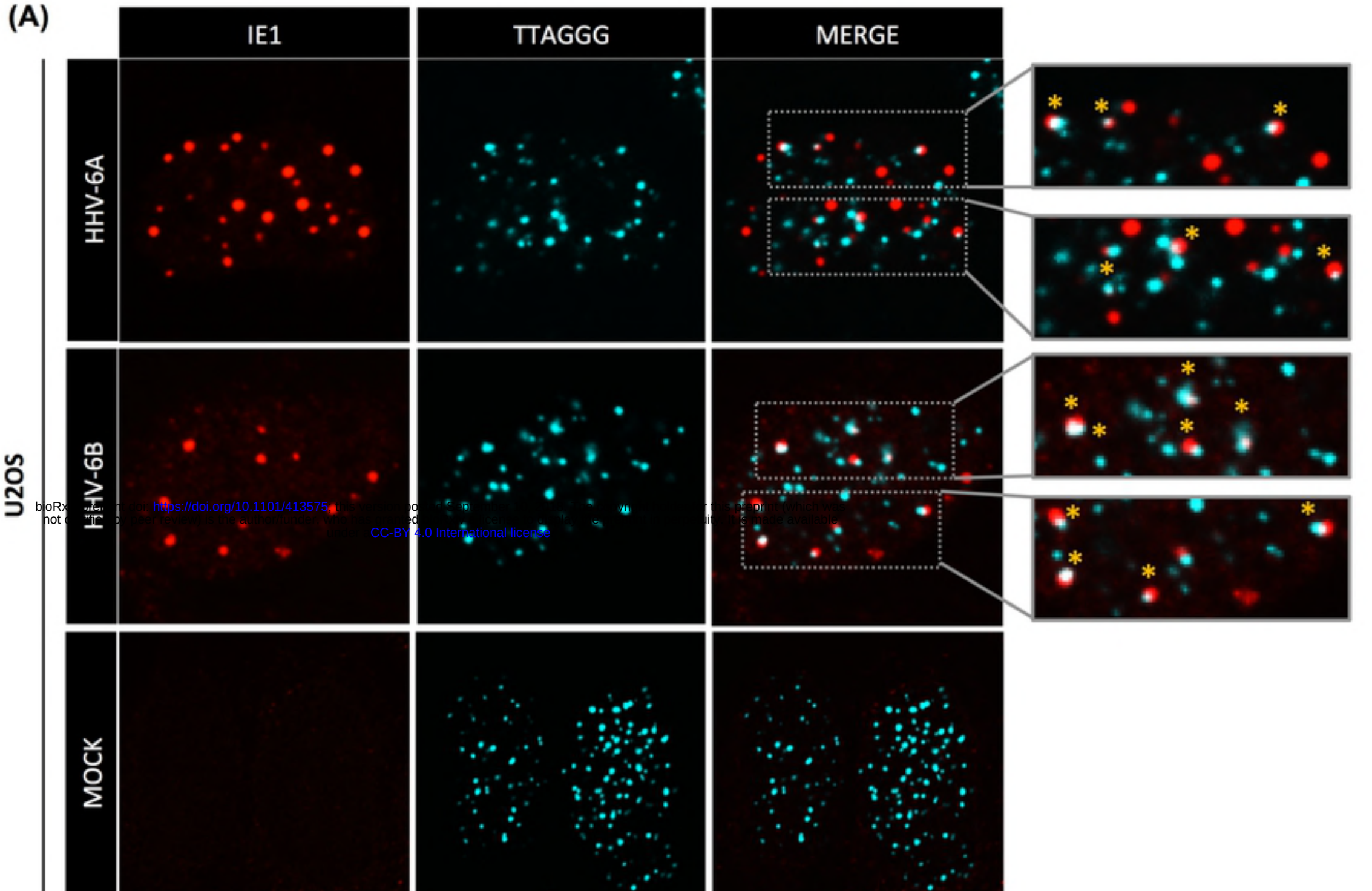

(B)

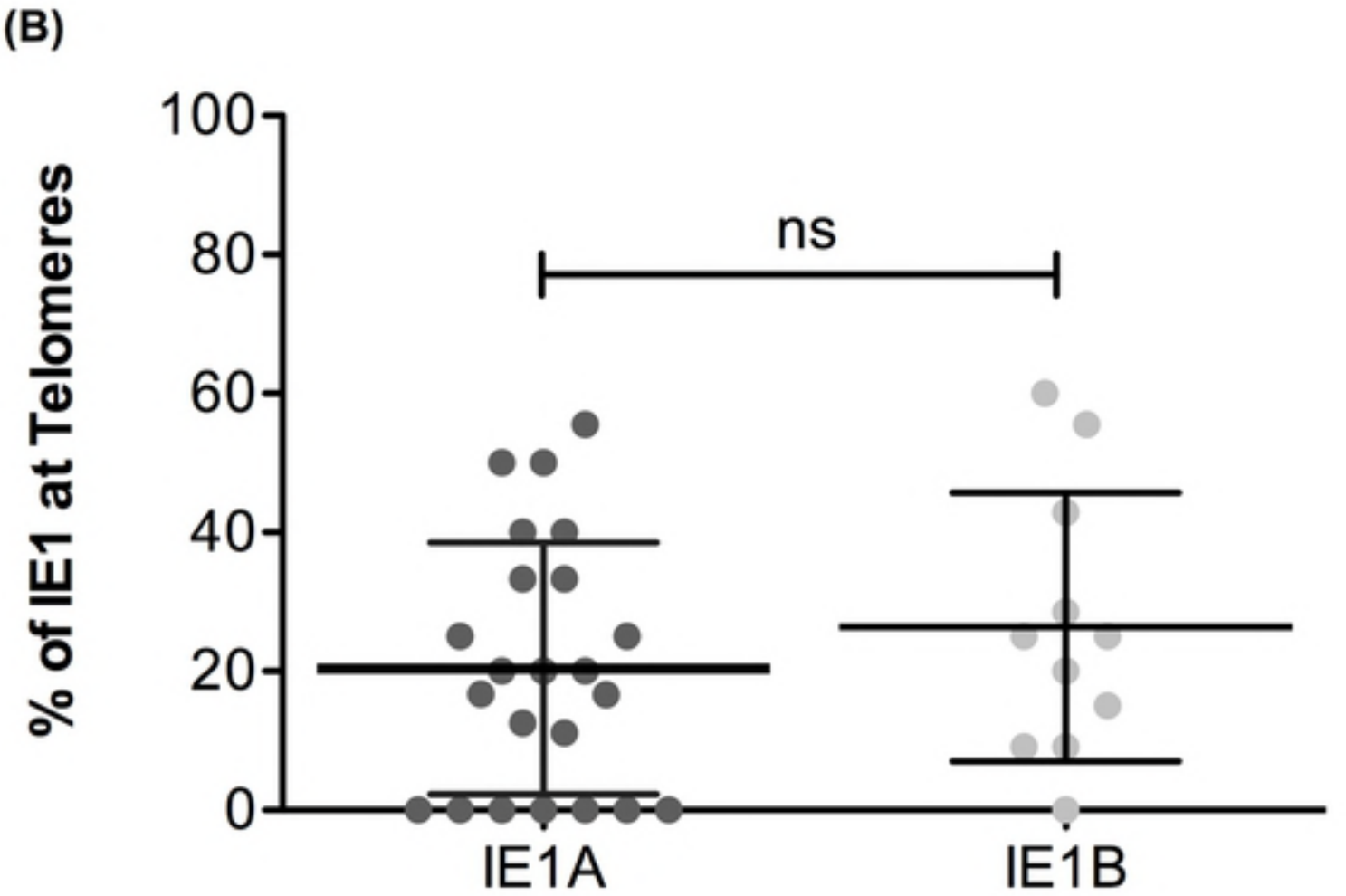

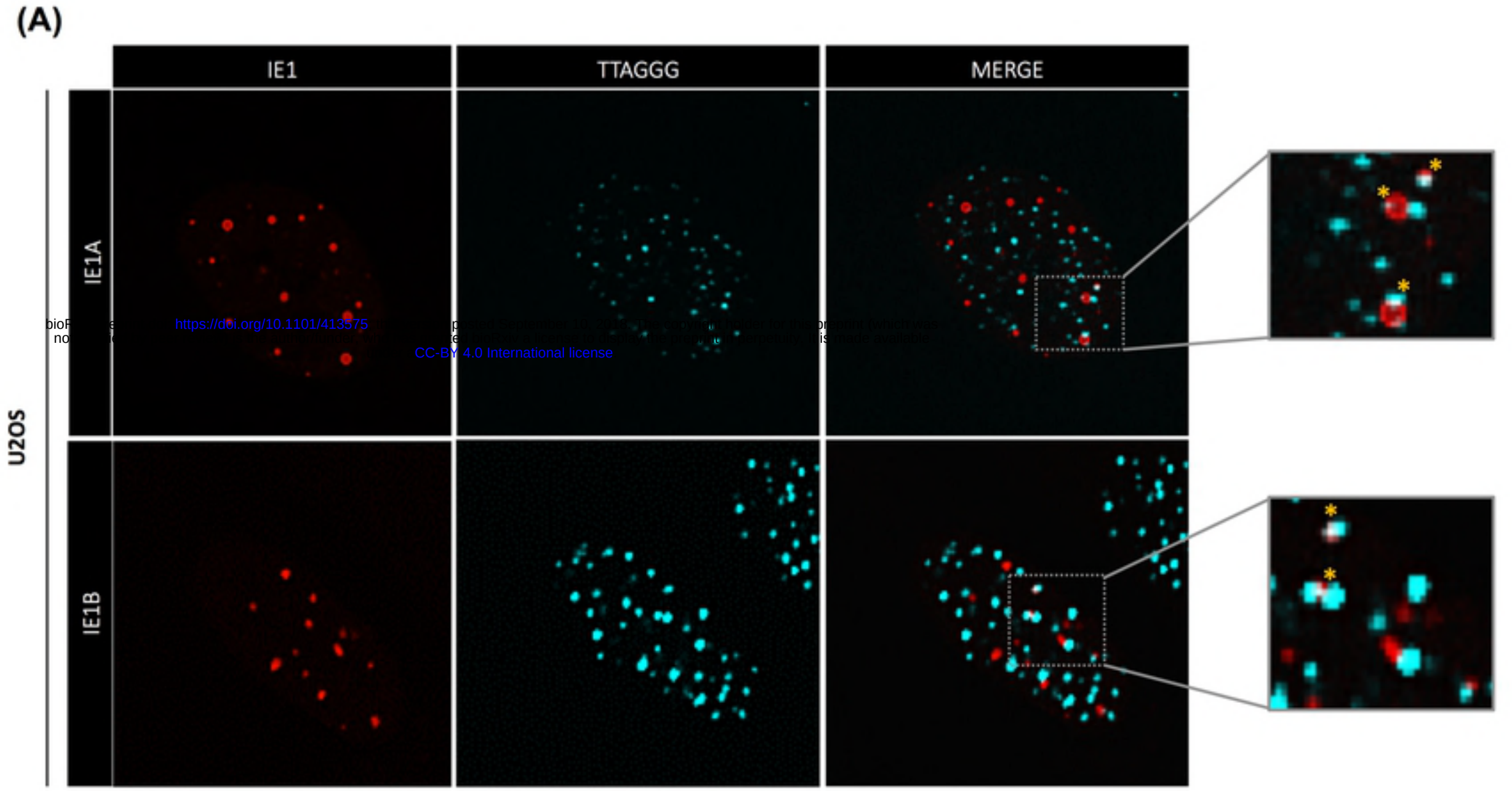

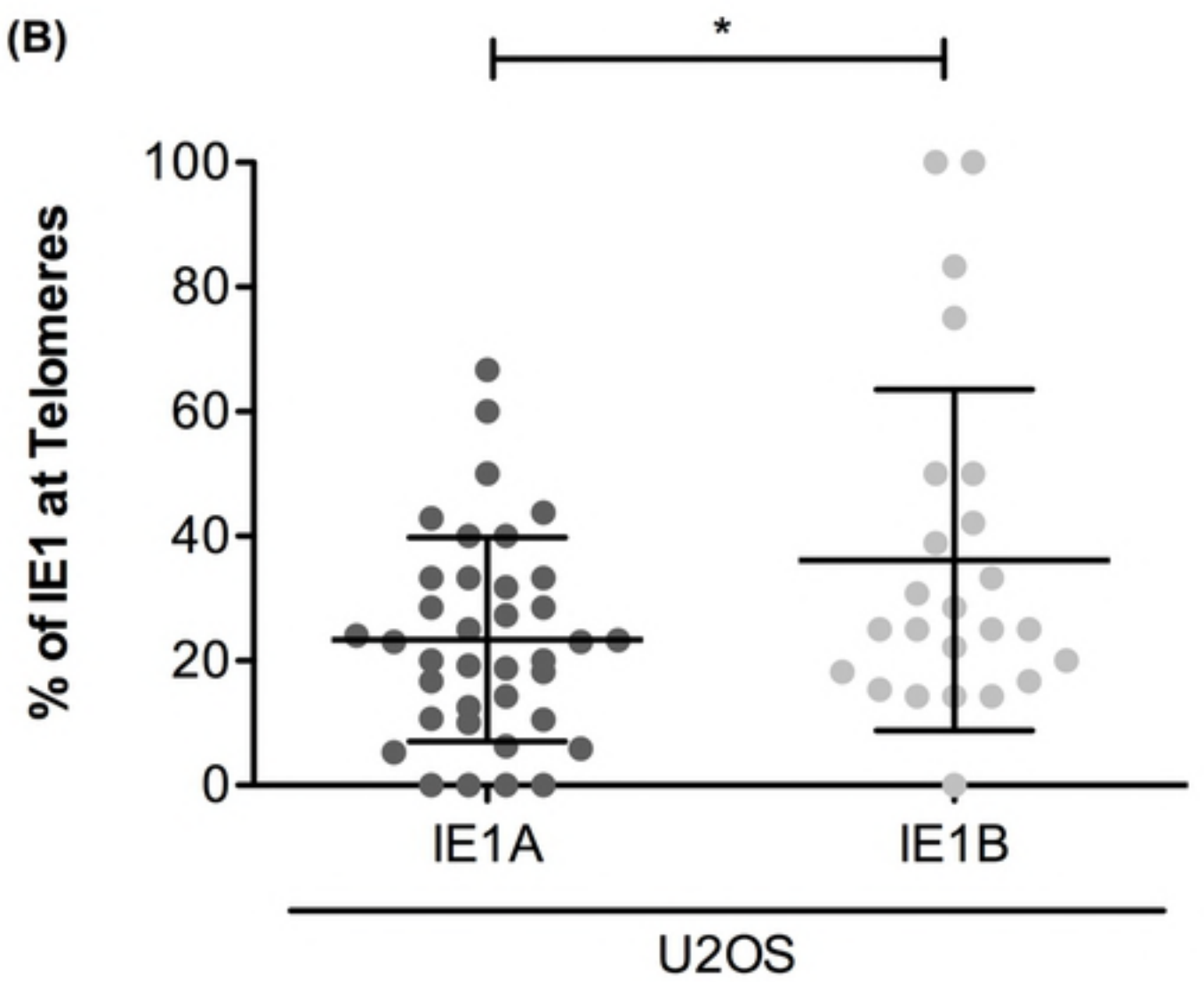

(A)

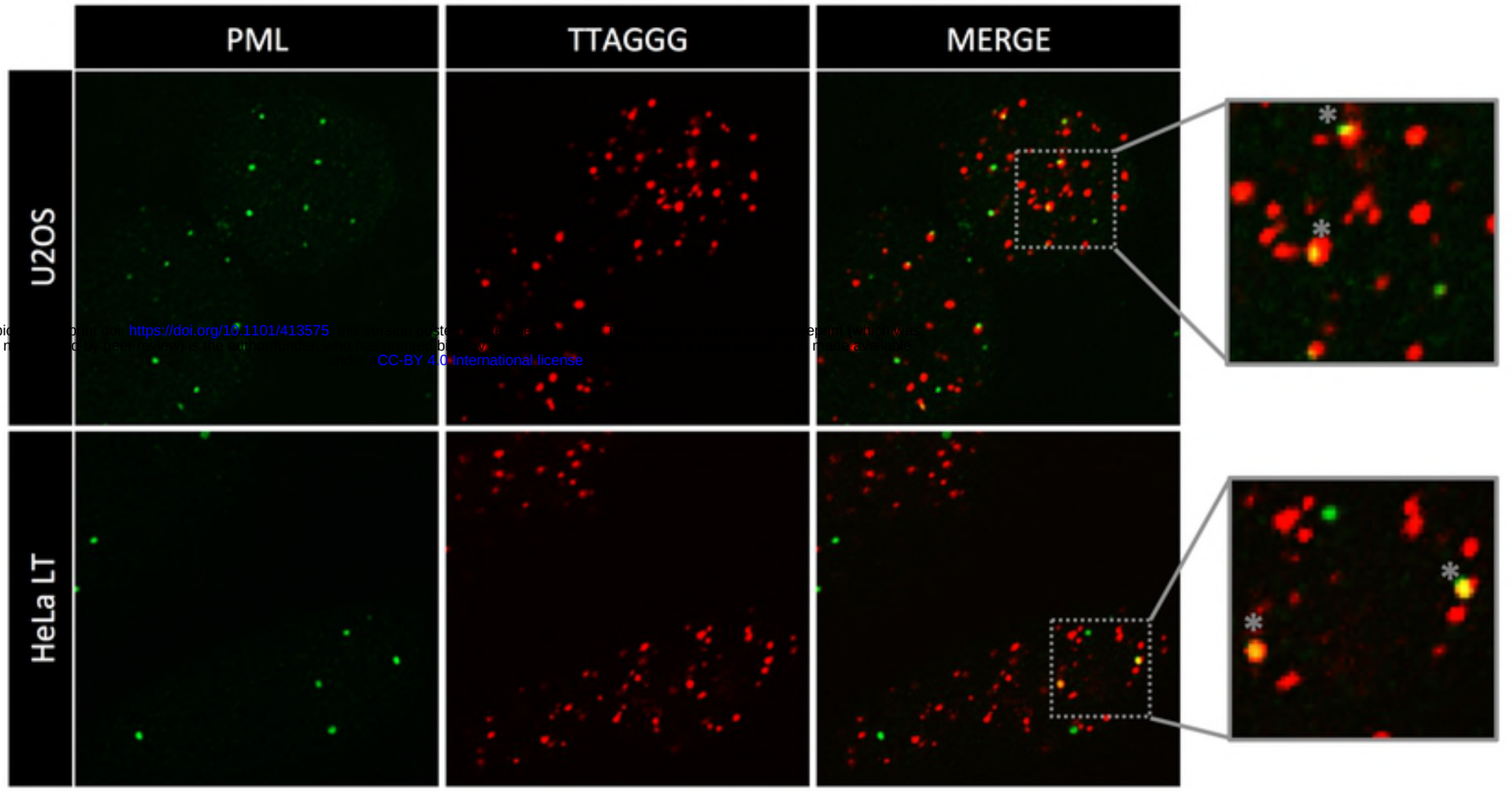

(B)

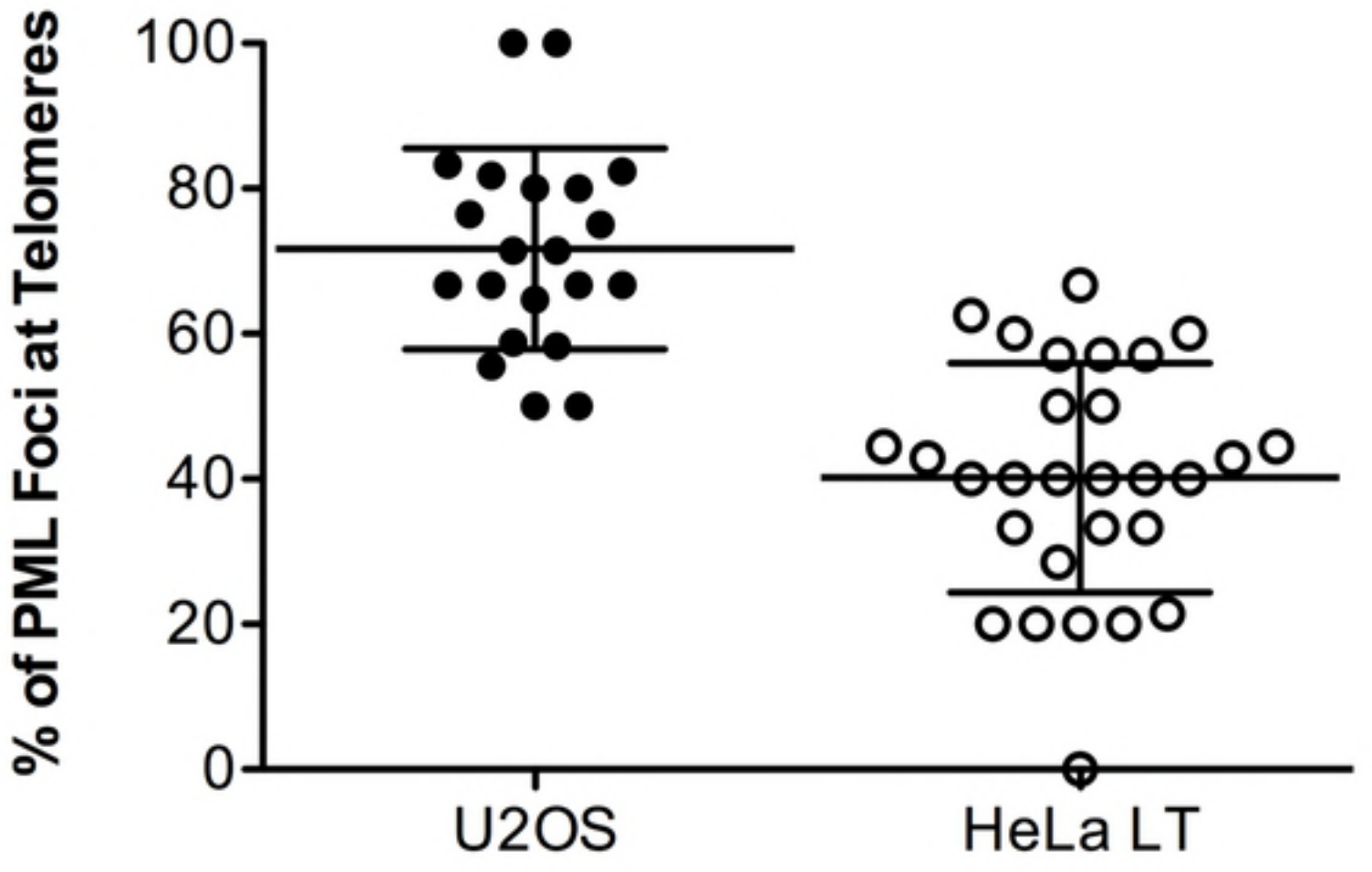

(A)

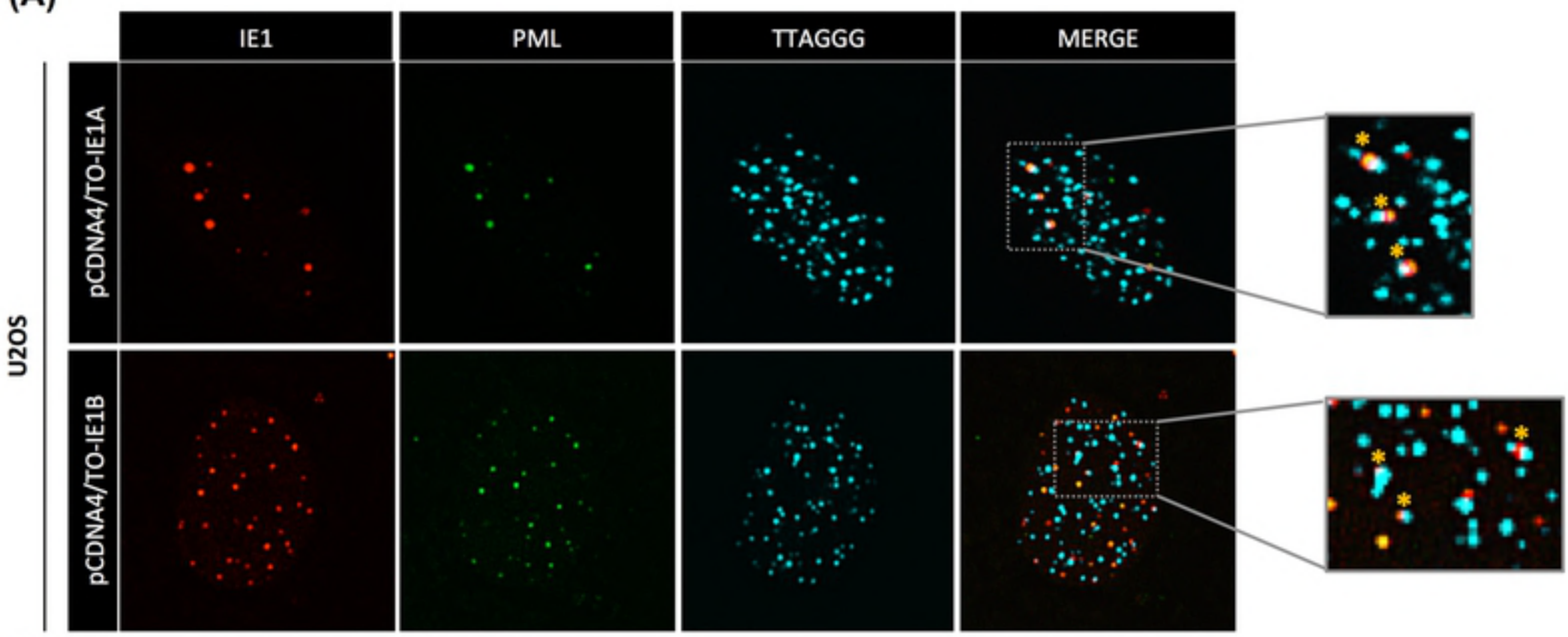

(B)

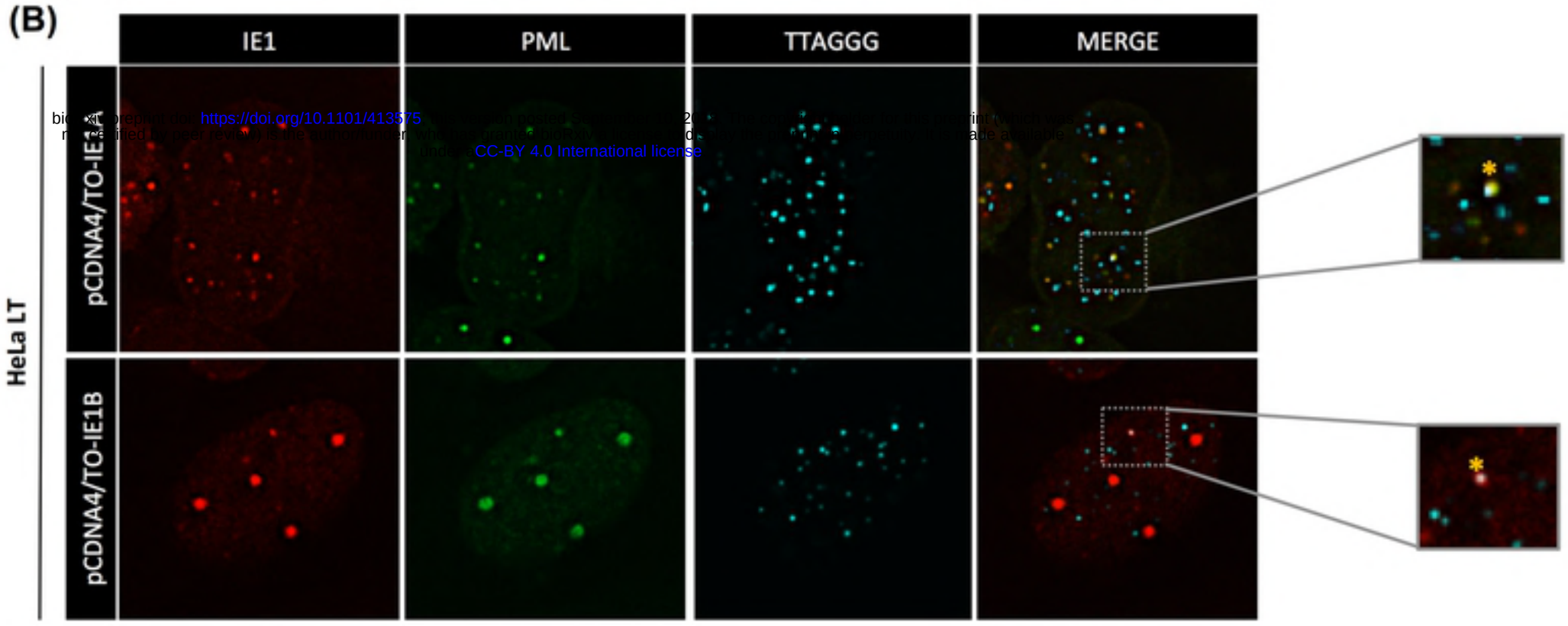

(C)

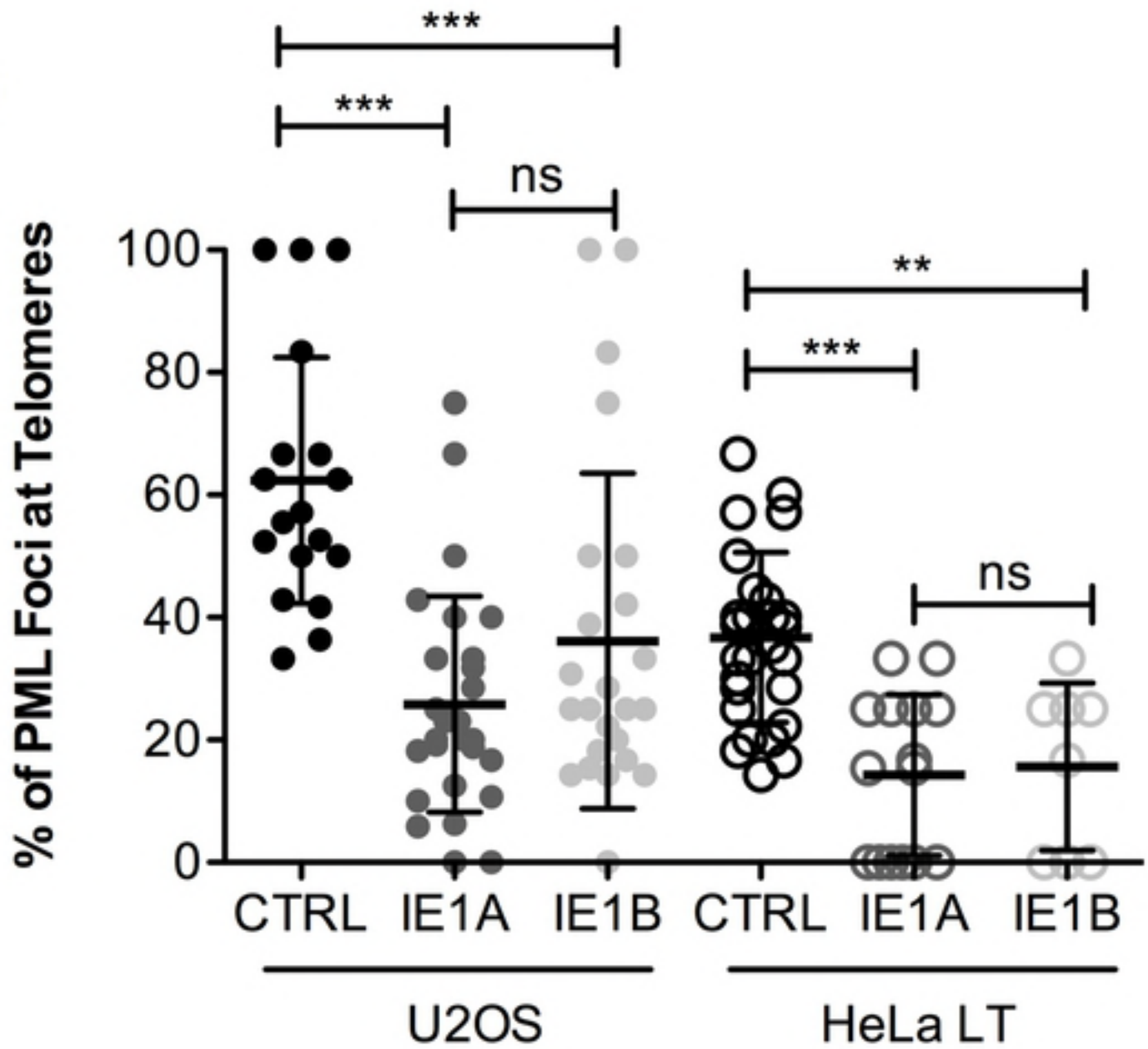

(A)

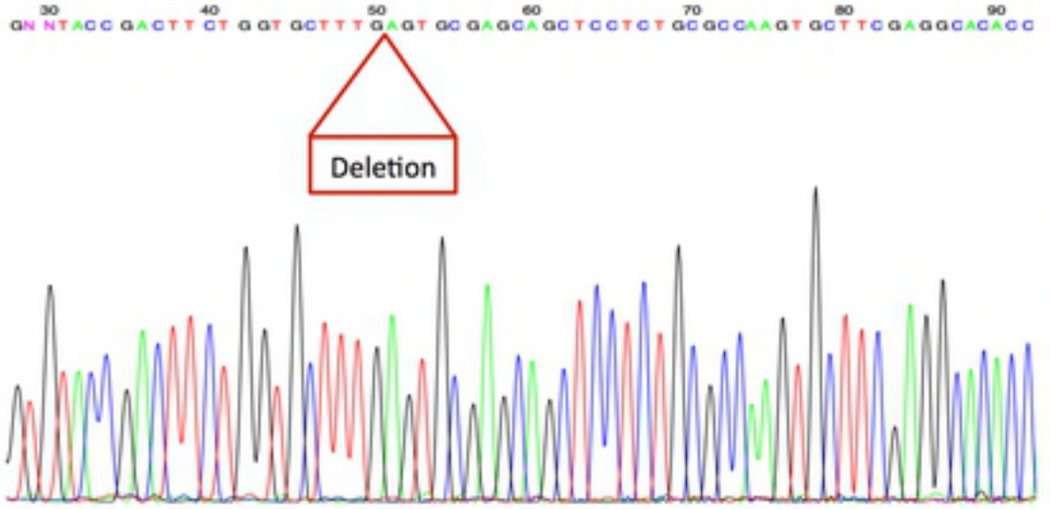

(B)

Met E P A P A R S P R P Q Q D P A R P Q E P T Met P P P E T P S E G R Q P S P S P S P T E R A P A S E E E F Q
F L R C Q Q C Q A E A K C P K L L P C L H T L C S G C L E A S G Met Q C P I C Q A P W P L G A D T P A L D N V
F F E S L Q R R L S V Y R Q I V D A Q A V C T R C K E S A D F W C F E C E Q L L C A K C F E A H Q W F L K H E A
R P L A E L R N Q S V R E F L D G T R K T N N I F C S N P N H R T P T L T S I Y C R G C S K P L C C S C A L L D S S
H S E L K C D I S A E I Q Q R Q E E L D A Met T Q A L Q E Q D S A F G A V H A Q Met H A A V G Q L G R A R A
E T E E L I R E R V R Q V V A H V R A Q E R E L L E A V D A R Y Q R D Y E E Met A S R L G R L D A V L Q R I R T
G S A L V Q R Met K C Y A S D Q E V L D Met H G F L R Q A L C R L R Q E E P Q S L Q A A V R T D G F D E F K
V R L Q D L S S C I T Q G K D A A V S K K A S P E A A S T P R D P I D V D L P E E A E R V K A Q V Q A L G L A E
A Q P Met A V V Q S V P G A H P V P V Y A F S I K G P S Y G E D V S N T T T A Q K R K C S Q T Q C P R K V I K
Met E S E E G K E A R L A R S S P E Q P R P S T S K A V S P P H L D G P P S P R S P V I G S E V F L P N S N H V
A S G A G E A G R E R N A L W Stop

Met E P A P A R S P R P Q Q D P A R P Q E P T Met P P P E T P S E G R Q P S P S P S P T E R A P A S E E E F Q
F L R C Q Q C Q A E A K C P K L L P C L H T L C S G C L E A S G Met Q C P I C Q A P W P L G A D T P A L D N V
F F E S L Q R R L S V Y R V L Stop V R A A P L R Q V L R G T P V V P Q A R G P A P S R A A Q P V G A Stop V P
G R H P Q D Q Q H L L L Q P Q P P H P Y A D Q H L L P R Met F Q A A V L L V R A P Stop

(C)

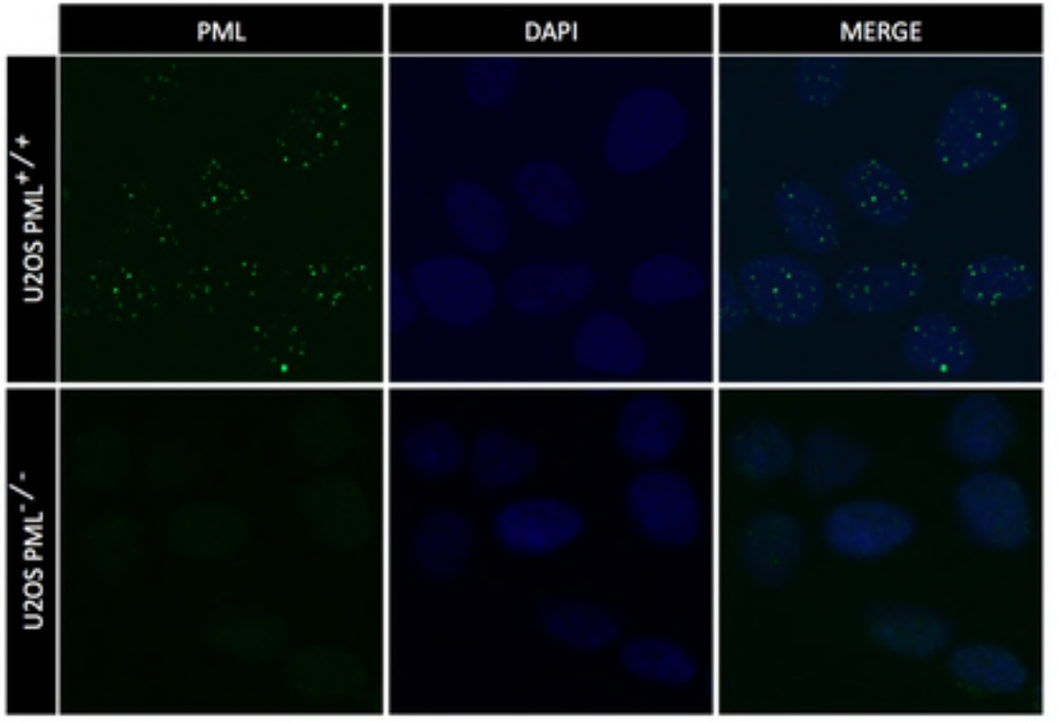

(D)

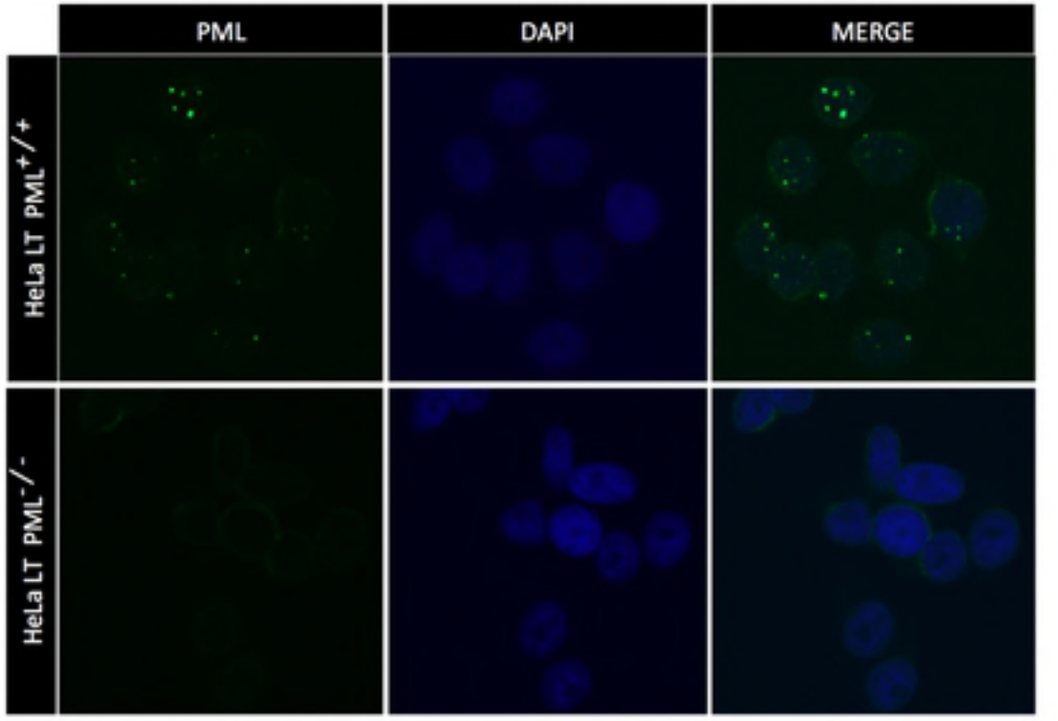

(A)

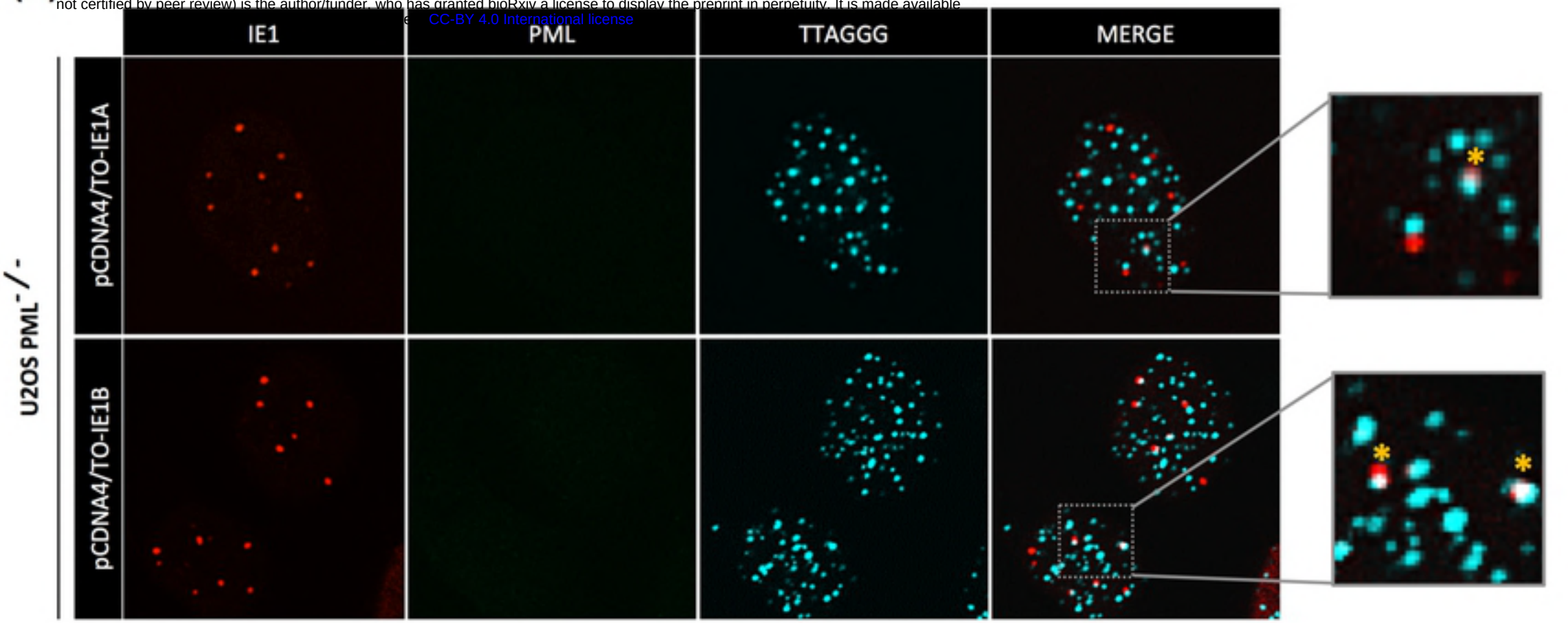

(B)

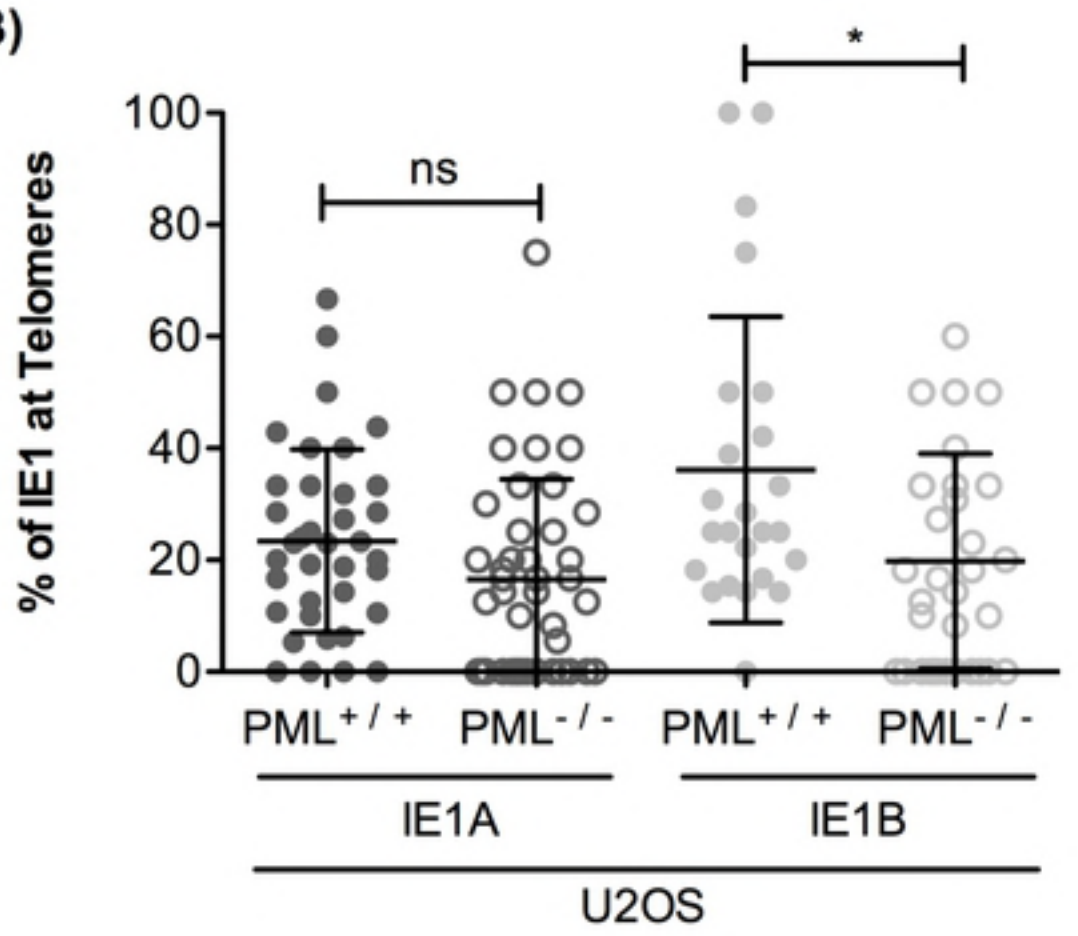

(A)

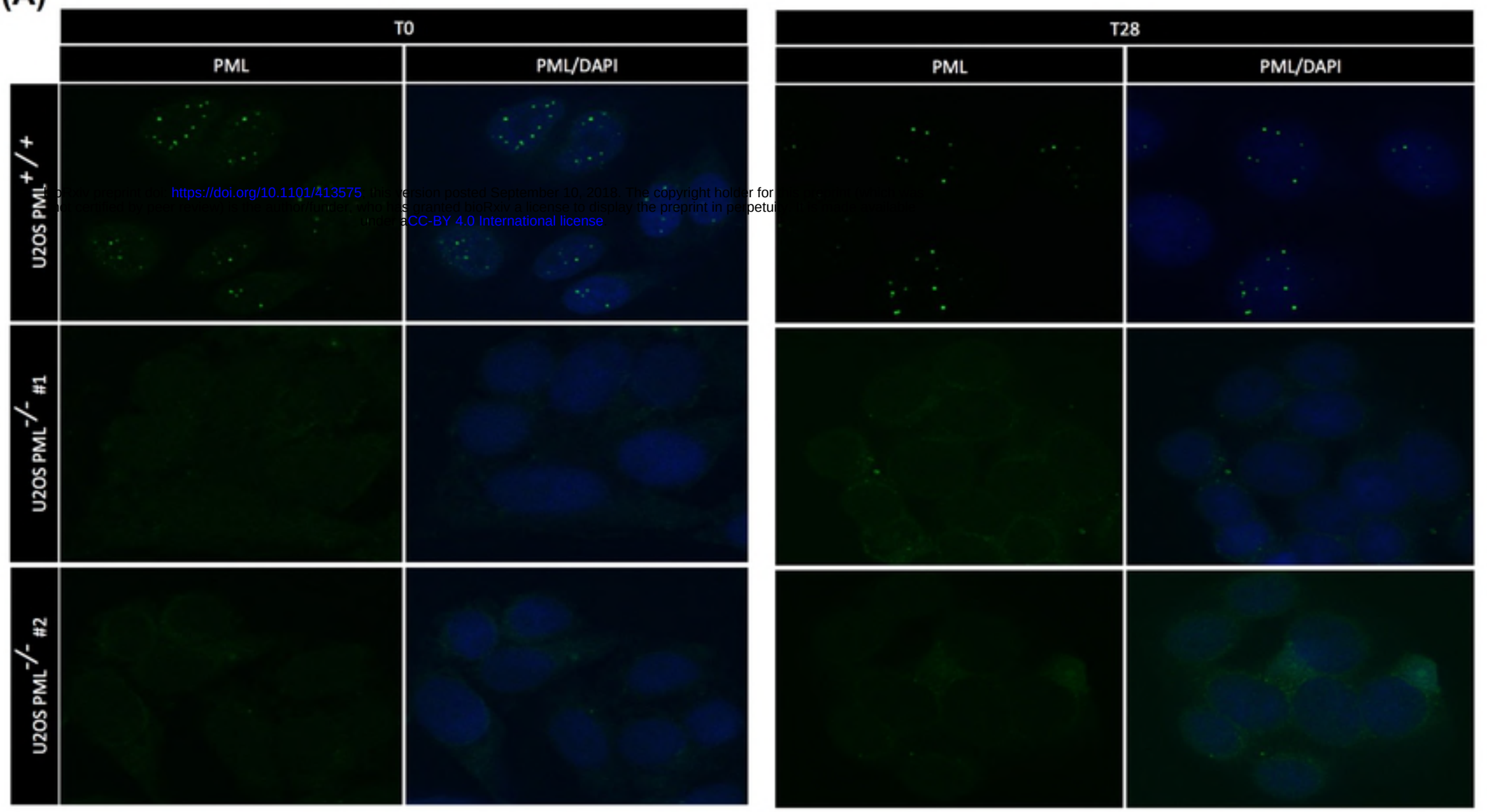

(B)

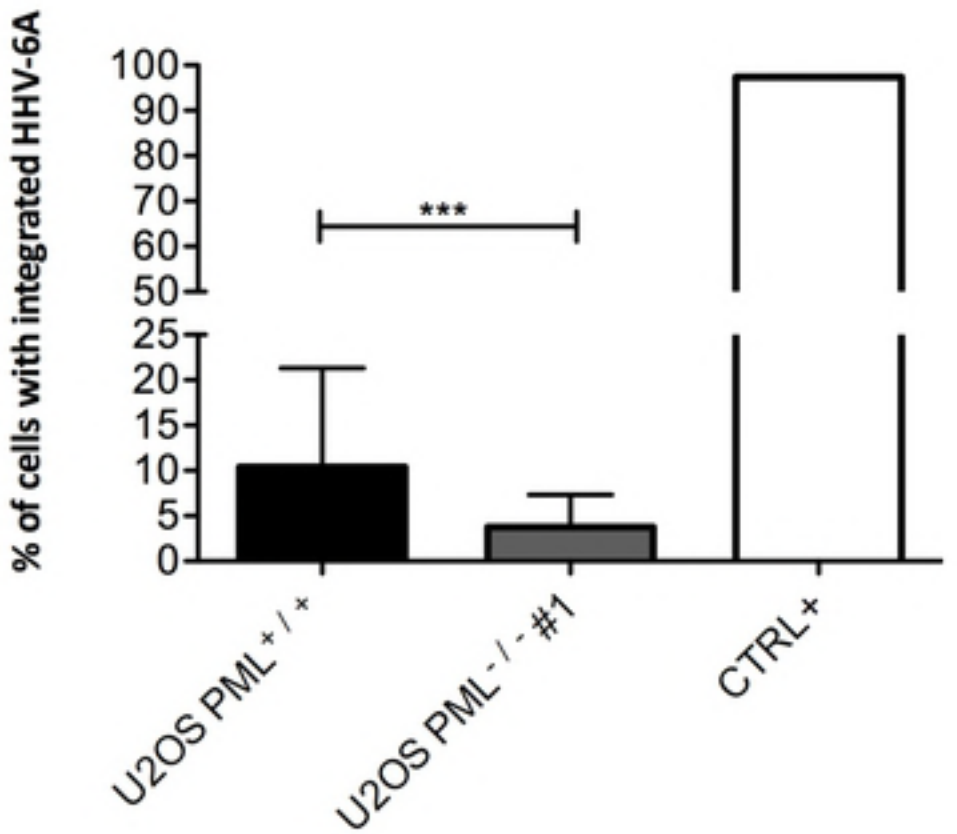

(C)

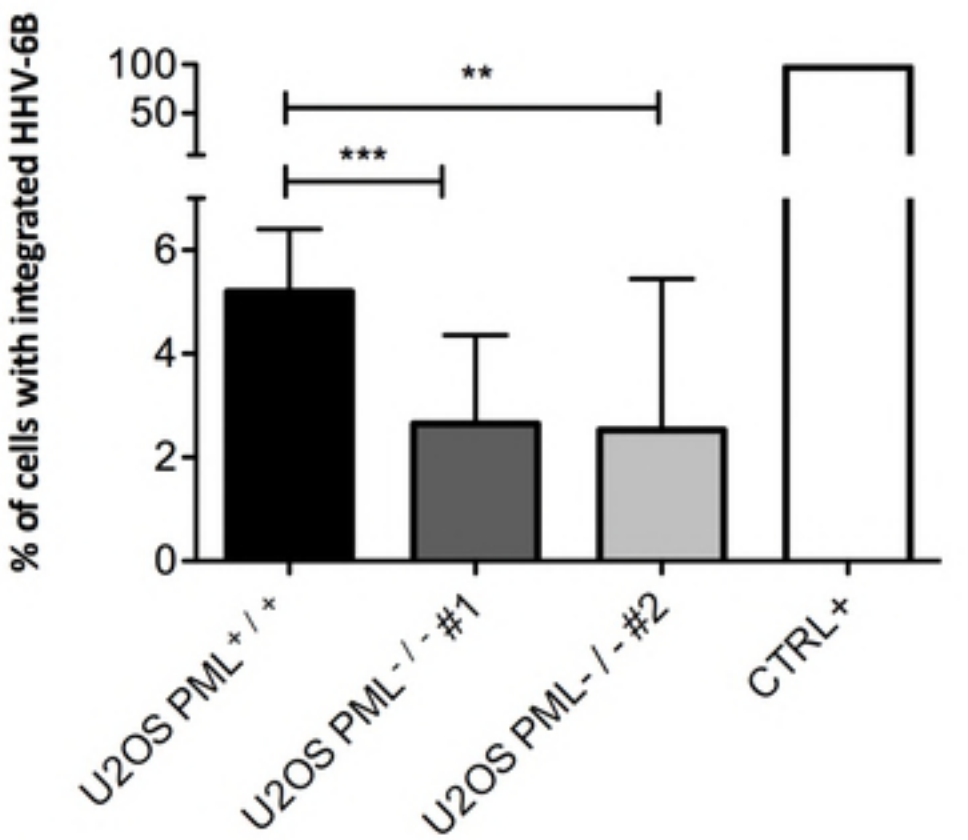

(A)

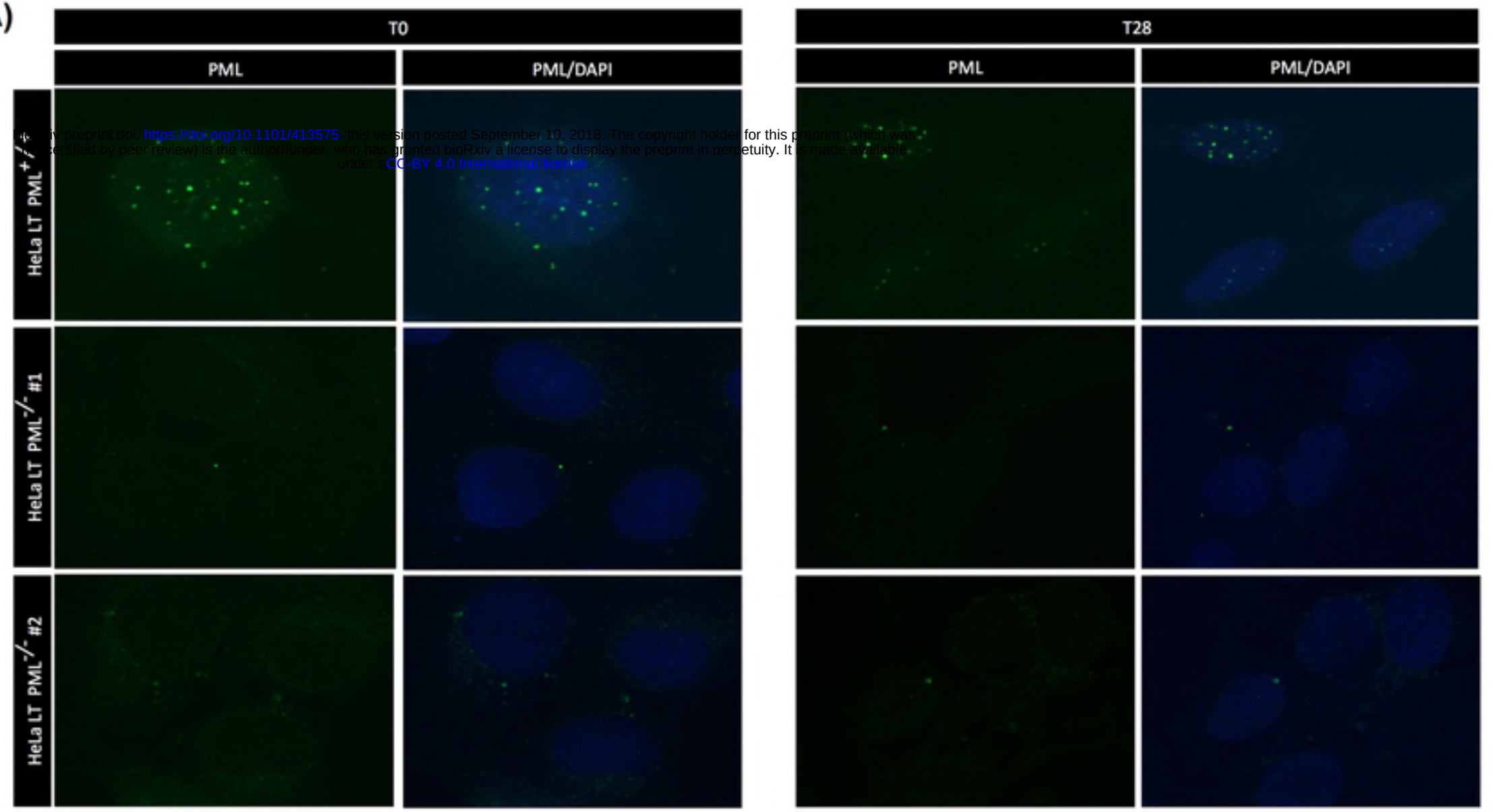

(B)

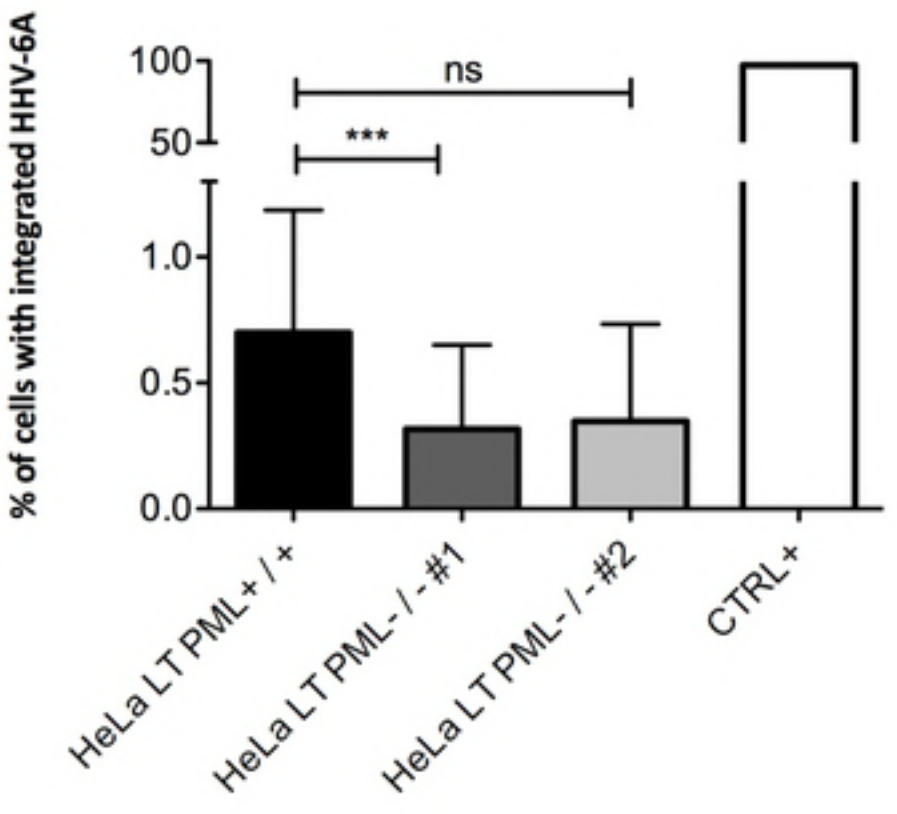

(C)

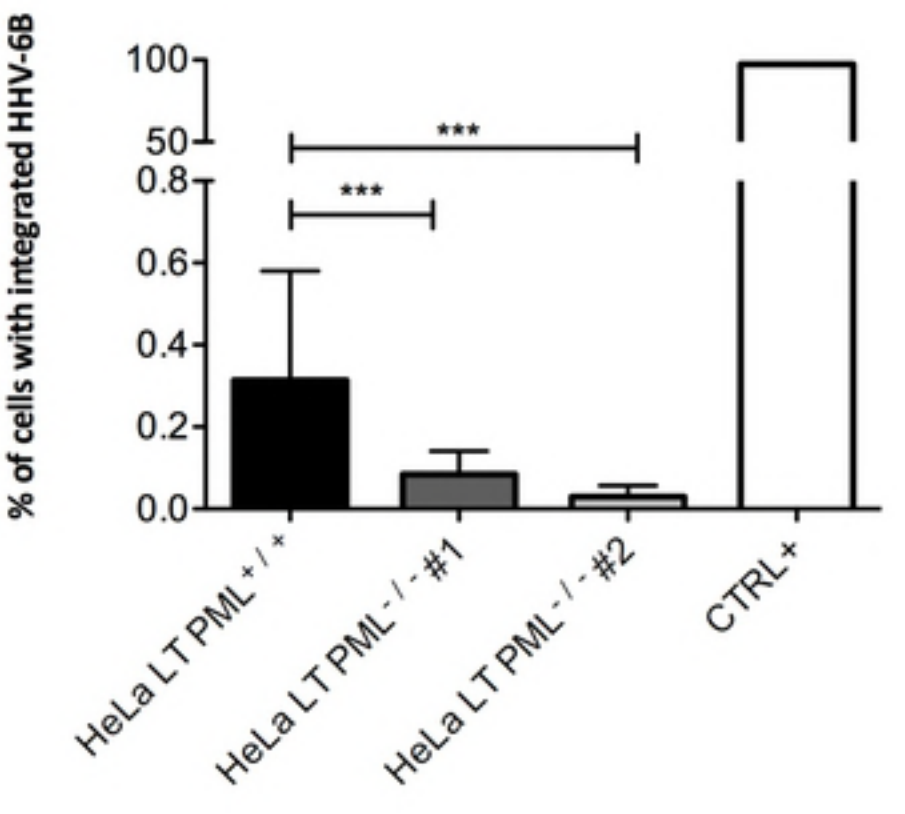

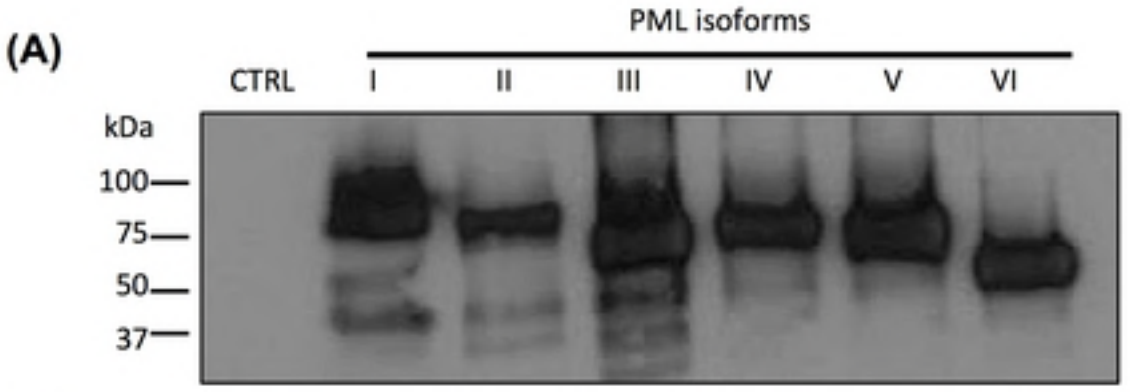

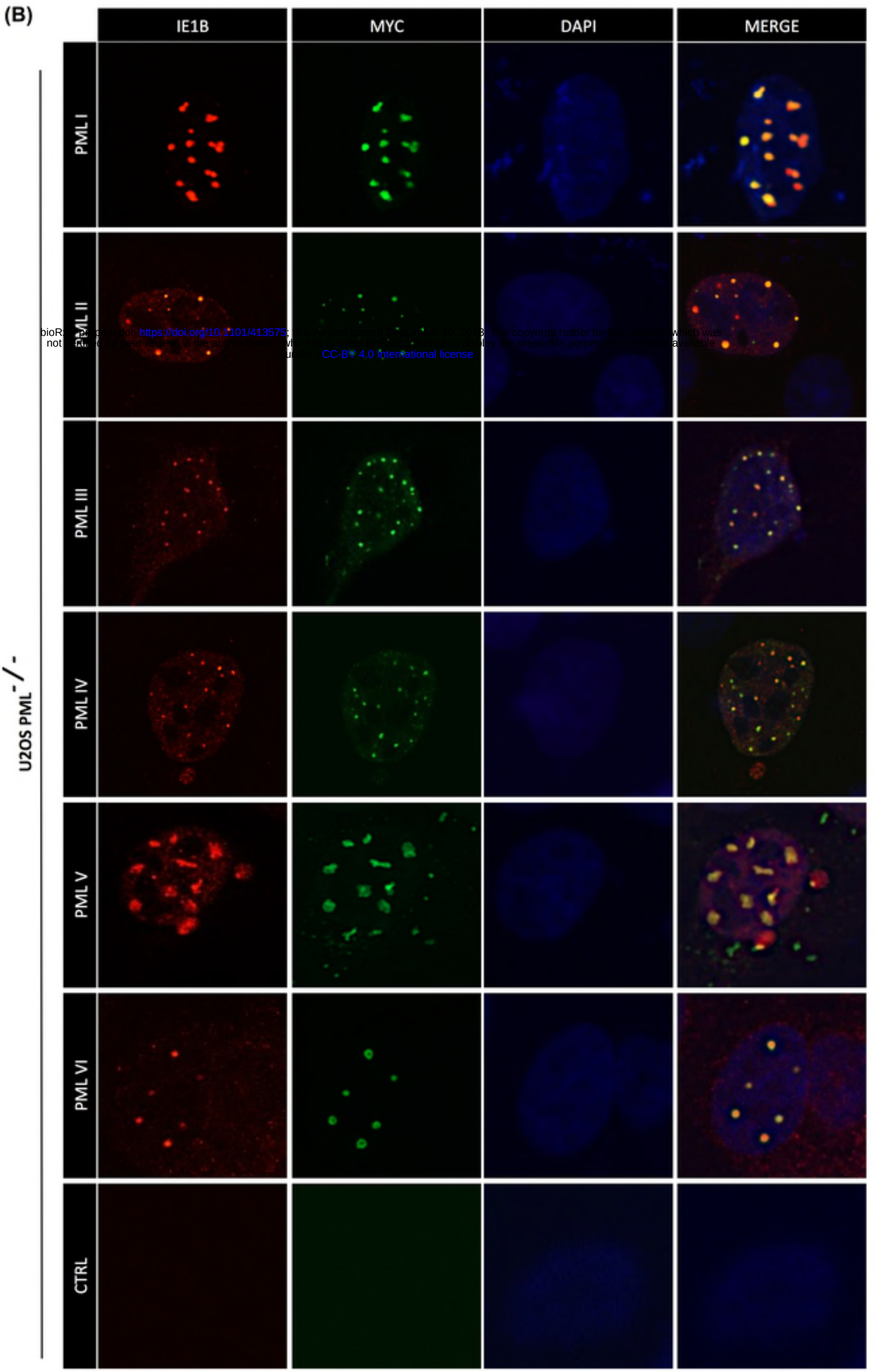

U2OS